arXiv:1109.3510v2 [cs.IT] 15 Aug 2012

Diversity Analysis of Bit-Interleaved Coded Multiple Beamforming with Orthogonal Frequency Division Multiplexing

Boyu Li, *Student Member, IEEE,* and Ender Ayanoglu, *Fellow, IEEE*

Abstract

Orthogonal Frequency Division Multiplexing (OFDM) has been combined with Multi-Input Multi-Output (MIMO) techniques for broadband wireless communication systems. Bit-Interleaved Coded Multiple Beamforming (BICMB) can achieve both spatial diversity and spatial multiplexing for MIMO flat fading channels. For MIMO frequency selective channels, BICMB with OFDM (BICMB-OFDM) can be applied to achieve both spatial diversity and multipath diversity, making it an important technique. However, analyzing the diversity of BICMB-OFDM is a challenging problem. In this paper, the diversity analysis of BICMB-OFDM is carried out. First, the maximum achievable diversity is derived and a full diversity condition $R_cSL \leq 1$ is proved, where R_c, S, and L are the code rate, the number of parallel streams transmitted at each subcarrier, and the number of channel taps, respectively. Then, the performance degradation due to the correlation among subcarriers is investigated. Finally, the subcarrier grouping technique is employed to combat the performance degradation and provide multi-user compatibility.

Index Terms

MIMO systems, Frequency division multiplexing, Singular value decomposition, Diversity methods, Convolutional codes, Correlation, Subcarrier multiplexing

I. INTRODUCTION

Substantial research and development interest have been drawn on Multiple-Input Multiple-Output (MIMO) systems because they provide high spectral efficiency and performance in a given bandwidth. In a MIMO system, beamforming techniques exploiting Singular Value Decomposition (SVD) are employed

---

B. Li and E. Ayanoglu are with the Center for Pervasive Communications and Computing, Department of Electrical Engineering and Computer Science, Henry Samueli School of Engineering, University of California, Irvine, CA 92697-3975 USA (e-mail: boyul@uci.edu; ayanoglu@uci.edu).

to achieve spatial multiplexing[1] and thereby increase the data rate, or to enhance performance, when the Channel State Information (CSI) is available at both the transmitter and receiver [3].

For flat fading channels, single beamforming carrying only one symbol at a time achieves full diversity [4], [5]. However, spatial multiplexing without channel coding results in the loss of the full diversity order. To overcome the performance degradation, Bit-Interleaved Coded Multiple Beamforming (BICMB) was proposed [6], [7], [8]. BICMB systems studied so far employ convolutional codes [9] as channel coding, and interleave the coded bit codewords through the multiple subchannels with different diversity orders. BICMB can achieve the full diversity order as long as the code rate R_c and the number of employed subchannels S satisfy the condition $R_cS \leq 1$ [10], [11].

If the channel is frequency selective, Orthogonal Frequency Division Multiplexing (OFDM) can be used to combat the Inter-Symbol Interference (ISI) caused by multipath propagation [12]. OFDM employs a large number of closely spaced orthogonal subcarrier signals to carry data, which are divided into several parallel data streams. In addition to its robustness against ISI, OFDM achieves many advantages such as easy adaptation to severe channel conditions without the computational burden of time-domain equalization, high spectral efficiency, efficient implementation using Fast Fourier Transform (FFT) and Inverse FFT (IFFT), and low sensitivity to time synchronization errors. Furthermore, multipath diversity can be achieved by adding channel coding [13], [14]. OFDM is well-suited for broadband data transmission, and it has been selected as the air interface for the Institute of Electrical and Electronics Engineers (IEEE) 802.11 Wireless Fidelity (WiFi) standard, the IEEE 802.16 Worldwide Interoperability for Microwave Access (WiMAX) standard, as well as the Third Generation Partnership Project (3GPP) Long Term Evolution (LTE) standard [15].

MIMO techniques have been incorporated with OFDM for all broadband wireless communication standards, i.e., WiFi [16], WiMax [17], and LTE [18]. Beamforming can be combined with OFDM for frequency selective MIMO channels to combat ISI and achieve spatial diversity [19]. Moreover, both spatial diversity and multipath diversity can be achieved by adding channel coding, e.g., BICMB with OFDM (BICMB-OFDM), [20], [21], [7]. Although some of the more modern standards employ more sophisticated codes [15], such as turbo codes and Low-Density Parity-Check (LDPC) codes [9], than convolutional codes employed by BICMB-OFDM, convolutional codes are important since they can be analyzed and there is a great deal of legacy products using them. Therefore, BICMB-OFDM is an important

---

[1] In this paper, the term “spatial multiplexing” is used to describe the number of spatial subchannels, as in [1]. Note that the term is different from “spatial multiplexing gain” defined in [2].

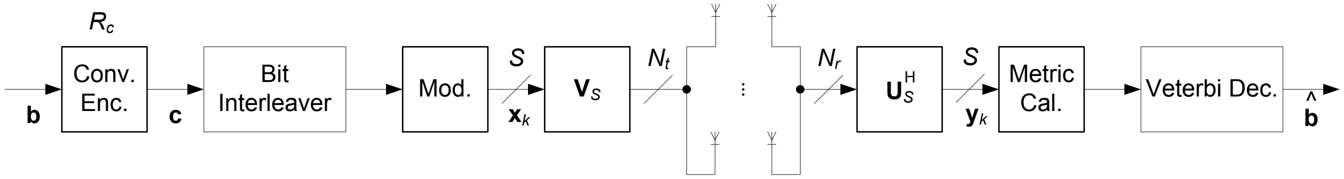

Fig. 1. Structure of BICMB.

technique for broadband wireless communication. However, the diversity analysis of BICMB-OFDM is a difficult challenge.

In this paper, the diversity analysis of BICMB-OFDM is carried out. First, the maximum achievable diversity is derived and the important α-spectra directly determining the diversity are introduced. Based on the analysis, a sufficient and necessary full diversity condition, $R_cSL \leq 1$ where S is the number of steams transmitted at each subcarrier and L is the number of channel taps, is proved. Then, the performance degradation caused by the correlation among subcarriers is investigated. To overcome the performance degradation, the subcarrier grouping technique [22], [23], [24] which also provides multi-user compatibility, is employed.

The remainder of this paper is organized as follows: Section II briefly describes BICMB and OFDM. In Section III, the system model of BICMB-OFDM is outlined. In Section IV, the maximum achievable diversity is derived, an important α-spectrum directly determining the diversity is introduced, and a sufficient and necessary condition to achieve full diversity is proved. Then, Section V investigates the performance degradation caused by the correlation among subcarriers and Section VI discusses the subcarrier grouping technique to combat the performance degradation and provide multi-user compatibility. In Section VII, simulation results are provided. Finally, a conclusion is provided in Section VIII.

II. BICMB AND OFDM

A. BICMB

For flat fading MIMO channels, the diversity of SVD beamforming is

$$D = (N_r - S + 1)(N_t - S + 1), \tag{1}$$

where N_r and N_t denote the number of transmit and receive antennas respectively and $S \leq \min\{N_t, N_r\}$ denote the number of streams transmitted at the same time [4]. BICMB was proposed to overcome the loss of full diversity N_rN_t for spatial multiplexing, i.e, $S > 1$ [6], [7], [8].

The structure of BICMB is presented in Fig. 1. First, the convolutional encoder of code rate R_c, possibly combined with a perforation matrix for a high rate punctured code [25], generates the bit codeword $\mathbf{c}$ from the information bits $\mathbf{b}$. Then, an interleaved bit sequence is generated by a bit interleaver before being modulated, e.g., Quadrature Amplitude Modulation (QAM), to a symbol sequence. Let N_r and N_t denote the number of transmit and receive antennas respectively. Assume that $S \leq \min\{N_t, N_r\}$ streams are transmitted at the same time. Hence, an $S \times 1$ symbol vector $\mathbf{x}_k$ is transmitted at the kth time instant.

The MIMO flat fading channel is assumed to be quasi-static and known by both the transmitter and the receiver, which is given by $\mathbf{H} \in \mathbb{C}^{N_r \times N_t}$, where $\mathbb{C}$ stands for the set of complex numbers. Then, the beamforming matrices are determined by SVD of $\mathbf{H}$, i.e., $\mathbf{H} = \mathbf{U}\mathbf{\Lambda}\mathbf{V}^H$, where $\mathbf{U}$ and $\mathbf{V}$ are unitary matrices, and $\mathbf{\Lambda}$ is a diagonal matrix whose sth diagonal element, $\lambda_s \in \mathbb{R}^+$, is a singular value of $\mathbf{H}$ in decreasing order with $s = 1, \ldots, S$, where $\mathbb{R}^+$ denotes the set of positive real numbers. When S streams are transmitted at the same time, the first S columns of $\mathbf{U}$ and $\mathbf{V}$, i.e., $\mathbf{U}_S$ and $\mathbf{V}_S$, are chosen to be used as beamforming matrices at the receiver and transmitter subcarrier, respectively. Therefore, the system input-output relation at the kth time instant is

$$y_{k,s} = \lambda_s x_{k,s} + n_{k,s}, \tag{2}$$

with $s = 1, \ldots, S$, where $y_{k,s}$ and $x_{k,s}$ are the sth element of the $S \times 1$ received symbol vector $\mathbf{y}_k$ and the transmitted symbol vector $\mathbf{x}_k$ respectively, and $n_{k,s}$ is the additive white complex Gaussian noise with zero mean.

The location of the coded bit $c_{k'}$ within the transmitted symbol is denoted as $k' \rightarrow (k, s, j)$, which means that $c_{k'}$ is mapped onto the jth bit position on the label of $x_{k,s}$. Let χ denote the signal set of the modulation scheme, and let χ_b^j denote a subset of χ whose labels have $b \in \{0, 1\}$ at the jth bit position. By using the location information and the input-output relation in (2), the receiver calculates the Maximum Likelihood (ML) bit metrics for $c_{k'} = b$ as

$$\Delta\left[y_{k,s}, c_{k'}\right] = \min_{x \in \chi_{c_{k'}}^j} \left|y_{k,s} - \lambda_s x\right|^2. \tag{3}$$

Finally, the ML decoder, which applies the soft-input Viterbi decoding [9] to find a codeword $\hat{\mathbf{c}}$ with the minimum sum weight and its corresponding information bit sequence $\hat{\mathbf{b}}$, uses the bit metrics calculated by (3) and makes decisions according to the rule given by [26] as

$$\hat{\mathbf{c}} = \arg\min_{\mathbf{c}} \sum_{k'} \Delta \left[y_{k,s}, c_{k'} \right]. \tag{4}$$

With a properly designed bit interleaver, the maximum achievable diversity of BICMB is given by [10], [11] as

$$D = (N_r - \lceil R_c S \rceil + 1)(N_t - \lceil R_c S \rceil + 1). \tag{5}$$

Based on (5), BICMB can achieve both full diversity and full multiplexing as long as the condition $R_c S \leq 1$ is satisfied.

B. OFDM

If the channel is frequency selective, OFDM can be used to combat the ISI caused by multipath propagation [12]. OFDM is a Frequency Division Multiplexing (FDM) scheme, whose subcarrier frequencies are chosen to be orthogonal to each other in order to remove the Inter-Carrier Interference (ICI) among subcarriers and provide high spectral efficiency.

The structure of OFDM is presented in Fig. 2. IFFT is used to multiplex the modulated symbols $\{x(1), \ldots, x(M)\}$ at the transmitter, where $x(m)$ denotes the modulated symbol transmitted by the mth subcarrier and M denotes the number of subcarriers. Hence, the output symbols of IFFT $\{\tilde{x}(1), \ldots, \tilde{x}(M)\}$ are calculated as

$$\tilde{x}(m) = \frac{1}{M} \sum_{k=1}^{M} x(k) e^{-i\frac{2\pi(m-1)k}{M}} \tag{6}$$

where $i = \sqrt{-1}$. Then, Cyclic Prefix (CP) $\{\tilde{x}(M - L_{cp} + 1), \ldots, \tilde{x}(M)\}$ is added before transmitting as guard interval, where L_{cp} denotes the length of CP and L_{cp} is no less than the number of channel taps L. The purpose of CP is to increase the OFDM symbol duration to eliminate ISI without breaking the orthogonality of transmitted symbols.

At the receiver, CP is removed from the received symbols $\{\tilde{y}(M - L_{cp} + 1), \ldots, \tilde{y}(M), \tilde{y}(1), \ldots, \tilde{y}(M)\}$. Then, FFT is used to derived the recovered symbols $\{y(1), \ldots, y(M)\}$ as

$$y(m) = \sum_{k=1}^{M} \tilde{y}(k) e^{-i\frac{2\pi(m-1)k}{M}}. \tag{7}$$

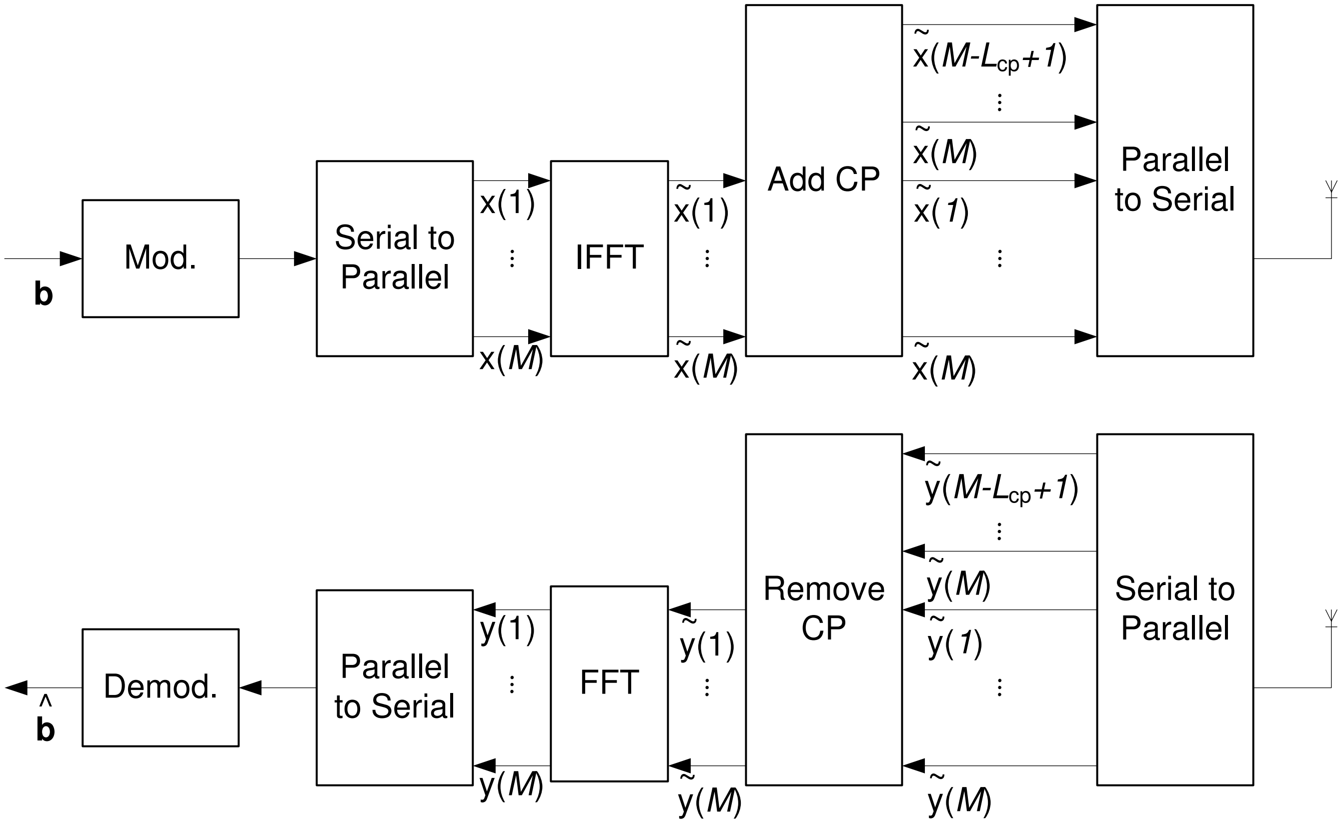

Fig. 2. Structure of OFDM.

The frequency selective channel with L taps is given by $\breve{h}(l) \in \mathbb{C}$ with $l = 1, \ldots, L$. Let

$$h(m) = \sum_{l=1}^{L} \breve{h}(l) e^{-i\frac{2\pi(m-1)\tau_l}{MT}} \tag{8}$$

denote the quasi-static flat fading channel observed at the mth subcarrier, where T denotes the sampling period and τ_l indicates the lth tap delay [27]. Then, the relation of $x(m)$ and $y(m)$ is given by

$$y(m) = h(m)x(m) + n(m), \tag{9}$$

where $n(m)$ is the additive white complex Gaussian noise with zero mean. As a result, symbol-by-symbol demodulation can be carried out for each subcarrier.

OFDM is robust against ISI and has small sensitivity to time synchronization errors. It can be efficiently implemented using FFT and IFFT, and easily adapted to severe channel conditions without the computational burden of time-domain equalization. It provides high spectral efficiency. Moreover, multipath diversity can be achieved by adding channel coding [13], [14]. The advantages of OFDM make it well-suited for broadband data transmission, and it has been selected as the air interface for all broadband

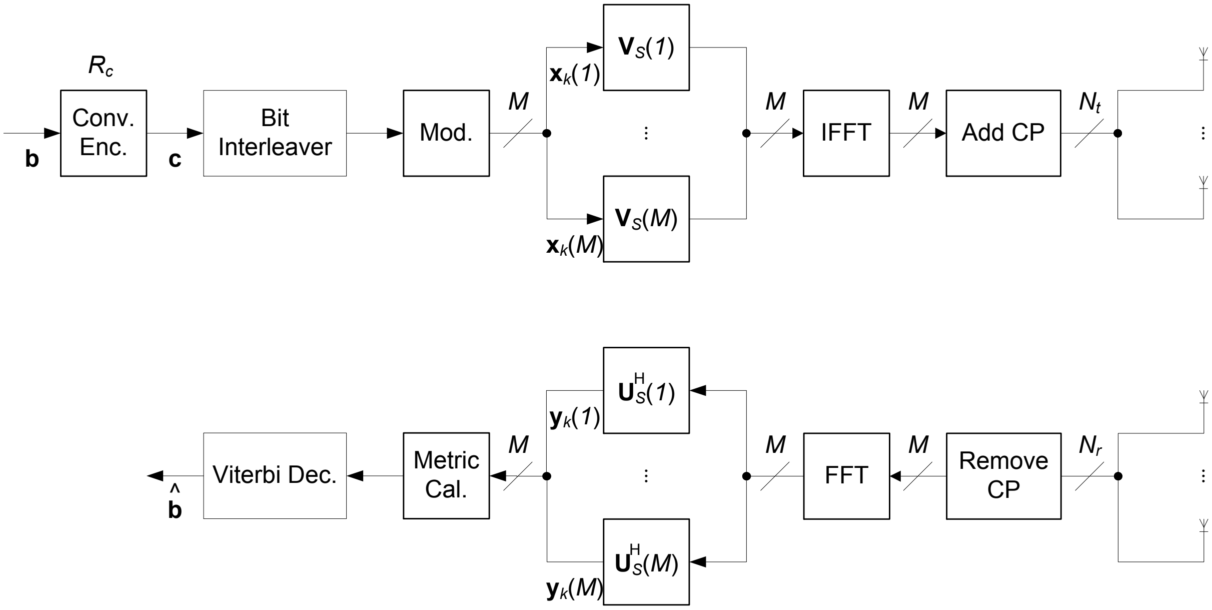

Fig. 3. Structure of BICMB-OFDM.

wireless communication standards, i.e., WiFi, WiMax, and LTE [15].

III. SYSTEM MODEL OF BICMB-OFDM

BICMB-OFDM was proposed to achieve both spatial diversity and multipath diversity for MIMO frequency selective channels, [20], [21], [7]. The structure of BICMB-OFDM is presented in Fig. 3. The channel coding, bit interleaver, and modulation of BICMB-OFDM are the same as BICMB introduced in section II-A. Assume that the modulated symbol sequence is transmitted through M subcarriers, and S streams are transmitted for each subcarrier at the same time. Hence, an $S \times 1$ symbol vector $\mathbf{x}_k(m)$ is transmitted through the mth subcarrier at the kth time instant with $m = 1, \ldots, M$.

The MIMO frequency selective channel with L taps is assumed to be quasi-static and known by both the transmitter and the receiver, which is given by $\breve{\mathbf{H}}(l) \in \mathbb{C}^{N_r \times N_t}$ with $l = 1, \ldots, L$. Let

$$\mathbf{H}(m) = \sum_{l=1}^{L} \breve{\mathbf{H}}(l) e^{-i\frac{2\pi(m-1)\tau_l}{MT}} \tag{10}$$

denote the quasi-static flat fading MIMO channel observed at the mth subcarrier. Then, SVD beamforming is carried out for each subcarrier. The beamforming matrices at the mth subcarrier are determined by $\mathbf{H}(m) = \mathbf{U}(m)\mathbf{\Lambda}(m)\mathbf{V}^H(m)$, where $\mathbf{U}(m)$ and $\mathbf{V}(m)$ are unitary matrices, and $\mathbf{\Lambda}(m)$ is the singular value matrix of $\mathbf{H}(m)$. When S streams are transmitted at the same time, the first S columns of $\mathbf{U}(m)$ and $\mathbf{V}(m)$, i.e., $\mathbf{U}_S(m)$ and $\mathbf{V}_S(m)$, are chosen to be used as beamforming matrices at the receiver and transmitter at the mth subcarrier, respectively.

The multiplication with beamforming matrices is carried out at each subcarrier before executing the Inverse Fast Fourier Transform (IFFT) and adding CP at the transmitter, and after executing the Fast Fourier Transform (FFT) and removing CP at the receiver, respectively. The length of CP is $L_{CP} \geq L$. Therefore, the system input-output relation for the mth subcarrier at the kth time instant is

$$y_{k,s}(m) = \lambda_s(m) x_{k,s}(m) + n_{k,s}(m), \tag{11}$$

with $s = 1, \ldots, S$, where $y_{k,s}(m)$ and $x_{k,s}(m)$ are the sth element of the $S \times 1$ received symbol vector $\mathbf{y}_k(m)$ and the transmitted symbol vector $\mathbf{x}_k(m)$ respectively, and $n_{k,s}(m)$ is the additive white complex Gaussian noise with zero mean and variance $N_0 = N_t/\gamma$ [28], with γ denoting the received Signal-to-Noise Ratio (SNR) over all the receive antennas. Note that the total transmitted power is scaled by N_t in order to make the received SNR γ.

Similarly to BICMB introduced in section II-A, the location of the coded bit $c_{k'}$ within the transmitted symbol is denoted as $k' \rightarrow (k, m, s, j)$, which means that $c_{k'}$ is mapped onto the jth bit position on the label of $x_{k,s}(m)$. By using the location information and the input-output relation in (11), the receiver calculates the ML bit metrics for $c_{k'} = b \in \{0, 1\}$ as

$$\Delta \left[y_{k,s}(m), c_{k'} \right] = \min_{x \in \chi^{j}_{c_{k'}}} \left| y_{k,s}(m) - \lambda_s(m) x \right|^2 . \tag{12}$$

Finally, the ML decoder, which applies the soft-input Viterbi decoding to find a codeword $\hat{\mathbf{c}}$ with the minimum sum weight and its corresponding information bit sequence $\hat{\mathbf{b}}$, uses the bit metrics calculated by (12) and makes decisions as

$$\hat{\mathbf{c}} = \arg\min_{\mathbf{c}} \sum_{k'} \Delta \left[y_{k,s}(m), c_{k'} \right] . \tag{13}$$

IV. MAXIMUM ACHIEVABLE DIVERSITY OF BICMB-OFDM

The performance of BICMB-OFDM is dominated by the instantaneous Pairwise Error Probability (PEP) with the worst diversity. Based on the bit metrics in (12), the instantaneous PEP of BICMB-OFDM between the transmitted bit codeword $\mathbf{c}$ and the decoded bit codeword $\hat{\mathbf{c}}$ is written as [7]

$$\Pr\left(\mathbf{c} \rightarrow \hat{\mathbf{c}}\right) = \mathrm{E}\left[\Pr\left(\mathbf{c} \rightarrow \hat{\mathbf{c}} \mid \mathbf{H}(m), \forall m\right)\right]$$

$$\leq \mathrm{E}\left[\frac{1}{2}\exp\left(-\frac{d_{min}^2\sum_{k',d_H}\lambda_s^2(m)}{4N_0}\right)\right], \tag{14}$$

where d_H denotes the Hamming distance between $\mathbf{c}$ and $\hat{\mathbf{c}}$, d_{min} is the minimum Euclidean distance in the constellation, $\sum_{k',d_H}$ stands for the summation of the d_H values corresponding to the different coded bits between the bit codewords.

Define an $M \times S$ matrix $\mathbf{A}$, whose element $\alpha_{m,s}$ denotes the number of distinct bits transmitting through the sth subchannel of the mth subcarrier for an error path, which implies $\sum_{m=1}^{M}\sum_{s=1}^{S}\alpha_{m,s} = d_H$. Let $\mathbf{a}_m^T$ denote the mth row of $\mathbf{A}$. Note that the α-spectrum here is similar to BICMB in the case of flat fading channels introduced in [10], [11]. Then (14) is rewritten as

$$\begin{aligned}\Pr\left(\mathbf{c}\rightarrow\hat{\mathbf{c}}\right) &\leq \mathrm{E}\left[\exp\left(-\frac{d_{min}^2\sum_m\sum_s\alpha_{m,s}\lambda_s^2(m)}{4N_0}\right)\right]\\ &\leq \mathrm{E}\left[\prod_m\exp\left(-\frac{d_{min}^2\sum_s\alpha_{m,s}\lambda_s^2(m)}{4N_0}\right)\right].\end{aligned} \tag{15}$$

In this section, the maximum achievable diversity is derived by considering the simplest case where no correlation exists among subcarriers. Note that correlation among subcarriers has a negative effect on the performance, which will be discussed in Section V.

Consider the case that different MIMO delay spread channels are uncorrelated and have equal power, and each element of each tap is statistically independent and modeled as a complex Gaussian random variable with zero mean and variance $1/L$, i.e.,

$$\mathrm{E}\left[\breve{h}_{u,v}(l)\breve{h}_{u,v}^*(l')\right] = \begin{cases} 0, & l \neq l', \\ \frac{1}{L}, & l = l', \end{cases} \tag{16}$$

where $\breve{h}_{u,v}(l)$ denotes the (u,v)th element in $\breve{\mathbf{H}}(l)$. Further consider that the channel taps are separated by a constant sampling time, i.e., $\tau_l = (l-1)T$ in (10). Then, the correlation between the mth subcarrier and the m'th subcarrier with $m \neq m'$ is given by

$$\begin{aligned}\rho &= \left|\frac{\mathrm{E}\left[h_{u,v}(m)h_{u,v}^*(m')\right]}{\sqrt{\mathrm{E}\left[h_{u,v}(m)h_{u,v}^*(m)\right]\mathrm{E}\left[h_{u,v}(m')h_{u,v}^*(m')\right]}}\right|\\ &= \left|\frac{\sum_{l=1}^{L}e^{-i\frac{2\pi(m-m')(l-1)}{M}}\mathrm{E}\left[\breve{h}_{u,v}(l)\breve{h}_{u,v}^*(l)\right]}{\sum_{l=1}^{L}\mathrm{E}\left[\breve{h}_{u,v}(l)\breve{h}_{u,v}^*(l)\right]}\right|\end{aligned}$$

$$= \frac{1}{L}\left|\sum_{l=1}^{L} e^{-i\frac{2\pi(m-m')(l-1)}{M}}\right|$$
$$= \frac{1}{L}\left|\frac{1-e^{-i\frac{2\pi(m-m')L}{M}}}{1-e^{-i\frac{2\pi(m-m')}{M}}}\right|. \tag{17}$$

Note that in the case of $L = M$, $\rho = 0$. This result implies that all subcarriers are uncorrelated. Note that $\mathbf{h}_{u,v} = [h_{u,v}(0), \ldots, h_{u,v}(M)]$ is a complex normal random vector, where $h_{u,v}(m)$ denotes the (u, v)th element in $\mathbf{H}(m)$. This implies that the components of $\mathbf{h}_{u,v}$ are independent if and only if they are uncorrelated [29]. Therefore, based on (17), all subcarriers are independent in the case of $L = M$. In the following part of this section, this special case is considered. Although this special case is not practical, its diversity analysis provides the maximum achievable diversity for the practical case. The reason is that correlation among subcarriers for the practical case has a negative effect on performance, which will be discussed in Section V.

Since subcarriers are independent in this special case, the singular value matrices $\mathbf{\Lambda}(m)$ are independent. Therefore, (15) is further rewritten as

$$\Pr\left(\mathbf{c} \rightarrow \hat{\mathbf{c}}\right) \leq \prod_{m} \mathrm{E}\left[\exp\left(-\frac{d_{min}^2 \sum_s \alpha_{m,s}\lambda_s^2(m)}{4N_0}\right)\right]. \tag{18}$$

For each subcarrier, the terms inside the expectation in (18) can be upper bounded by employing the theorem proved in [30], which is given below.

Theorem 1. *Consider the largest $S \leq \min\{N_t, N_r\}$ eigenvalues μ_s of the uncorrelated central $N_r \times N_t$ Wishart matrix [31] that are sorted in decreasing order, and a weight vector $\boldsymbol{\eta} = [\eta_1, \cdots, \eta_S]^T$ with non-negative real elements. In the high SNR regime, an upper bound for the expression $E[\exp(-\gamma \sum_{s=1}^{S} \eta_s\mu_s)]$, which is used in the diversity analysis of a number of MIMO systems, is*

$$E\left[\exp\left(-\gamma\sum_{s=1}^{S}\eta_s\mu_s\right)\right] \leq \zeta\left(\eta_{min}\gamma\right)^{-(N_r-\delta+1)(N_t-\delta+1)}, \tag{19}$$

where γ is SNR, ζ is a constant, $\eta_{min} = \min_{\eta_i\neq 0}\{\eta_i\}_{i=1}^{S}$, and δ is the index to the first non-zero element in the weight vector.

Proof: See [30]. □

By applying Theorem 1 to (18), an upper bound of PEP is

$$\Pr\left(\mathbf{c} \to \hat{\mathbf{c}}\right) \leq \prod_{m,\mathbf{a}_m \neq \mathbf{0}} \zeta_m \left(\frac{d_{min}^2 \alpha_{m,min}}{4N_t} \gamma \right)^{-D_m}, \tag{20}$$

with $D_m = (N_r - \delta_m + 1)(N_t - \delta_m + 1)$, where $\alpha_{m,min}$ denotes the first non-zero element in $\mathbf{a}_m$, δ_m denotes the index of $\alpha_{m,min}$ in $\mathbf{a}_m$, and ζ_m is a constant. Therefore, the diversity can be easily found from (20), which is

$$D = \sum_{m,\mathbf{a}_m \neq \mathbf{0}} D_m. \tag{21}$$

Because the error path with the worst diversity order dominates the performance, the results of (20) and (21) show that the maximum achievable diversity of BICMB-OFDM is directly decided by the α-spectra. Note that the α-spectra are related with the bit interleaver and the trellis structure of the convolutional code, and they can be derived by a similar approach to BICMB in the case of flat fading channels presented in [10], or by computer search.

An example is provided here to show the relation between the α-spectra and the diversity. Consider the parameters $N_t = N_r = S = L = M = 2$. Assume that the $R_c = 1/2$ convolutional code with generator polynomial $(5, 7)$ in octal is employed, and the bit interleaver applies simple bit rotation, i.e., the sth bit of the mth S bits are transmitted through the sth subchannels at the mth subcarrier at one time instant. In this case, the dominant error path has the α-spectrum $\mathbf{A} = [0\,1;\, 2\,2]$, which implies that $\delta_1 = 2$ and $\delta_2 = 1$. Hence, $D_1 = 1$, $D_2 = 4$. Therefore, the maximum achievable diversity order is $D = D_1 + D_2 = 5$.

A. α-spectra

A method to derive the α-spectra is illustrated by the following simple example. For this example, the system is composed of a 4-state $1/2$-rate convolutional encoder and a spatial de-multiplexer rotating with an order of a, b, c, and d which represent the four streams of transmission. Fig. 4 represents a trellis diagram of this convolutional encoder for one period at the steady state. Since a convolutional code is linear, the all-zeros codeword is assumed to be the input to the encoder. To find a transfer function of a convolutional code and a spatial de-multiplexer, the branches are labeled as a combination of a^{β_a}, b^{β_b}, c^{β_c}, and d^{β_d}, where the exponent denotes the number of usage of each subchannel which contributes to detecting the wrong branch by the detector. Additionally, Z^{β_Z}, whose exponent satisfies $\beta_Z = \beta_a + \beta_b + \beta_c + \beta_d$, is included to get the relationship between the Hamming distance d_H and α-spectrum of an error event.

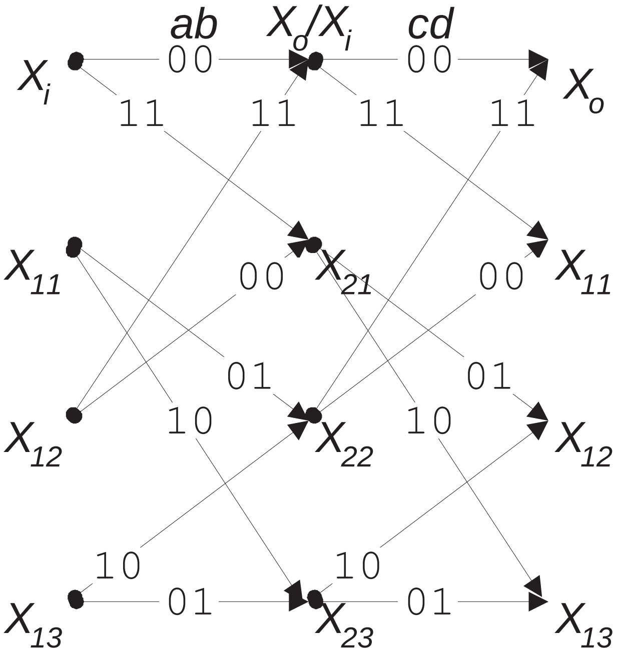

Fig. 4. Trellis of 4-state $1/2$-rate convolutional code with 4 streams

Furthermore, the non-zero states are symbolically labeled from X_{11} to X_{23} as in Fig. 4, while the zero state is labeled as X_i if branches split and X_o if branches merge, also as shown in Fig. 4.

Define $\mathbf{x} = [X_{11},\ X_{12},\ X_{13},\ \ X_{21},\ \ X_{22},\ \ X_{23}]^T$. Then, the state equations are given by the matrix equation

$$\mathbf{x} = \mathbf{F}\mathbf{x} + \mathbf{t}X_i = \begin{bmatrix} 0 & 0 & 0 & 0 & 1 & 0 \\ 0 & 0 & 0 & dZ & 0 & cZ \\ 0 & 0 & 0 & cZ & 0 & dZ \\ 0 & 1 & 0 & 0 & 0 & 0 \\ bZ & 0 & aZ & 0 & 0 & 0 \\ aZ & 0 & bZ & 0 & 0 & 0 \end{bmatrix} \mathbf{x} + \begin{bmatrix} cdZ^2 \\ 0 \\ 0 \\ abZ^2 \\ 0 \\ 0 \end{bmatrix} X_i. \tag{22}$$

We also get

$$X_o = \mathbf{g}\mathbf{x} = \begin{bmatrix} 0 & abZ^2 & 0 & 0 & cdZ^2 & 0 \end{bmatrix} \mathbf{x}. \tag{23}$$

The transfer function is represented in closed form by using the method in [25] as

$$\begin{aligned} \mathbf{T}(a,b,c,d,Z) &= \mathbf{g}\left[\mathbf{I} - \mathbf{F}\right]^{-1}\mathbf{t} \\ &= \mathbf{g}\mathbf{t} + \sum_{u=1}^{\infty} \mathbf{g}\mathbf{F}^u\mathbf{t} \end{aligned}$$

$$
\begin{aligned}
&= Z^5(a^2b^2d + bc^2d^2)\\
&\quad + Z^6(2a^2bc^2d + a^2b^2d^2 + b^2c^2d^2)\\
&\quad + Z^7(a^2b^3c^2 + 2a^2b^2c^2d + 2a^2bc^2d^2 +\\
&\qquad\qquad b^3c^2d^2 + a^2b^2d^3 + a^2c^2d^3)\\
&\quad + Z^8(a^4b^2c^2 + 4a^2b^3c^2d + 4a^2b^2c^2d^2 +\\
&\qquad\qquad b^4c^2d^2 + a^2c^4d^2 + 4a^2bc^2d^3 + a^2b^2d^4) + \cdots
\end{aligned} \tag{24}
$$

where $[\mathbf{I} - \mathbf{F}]^{-1}$ can be expanded as $\mathbf{I} + \mathbf{F} + \mathbf{F}^2 + \cdots$ through an infinite series of power of matrices.

Consider BICMB-OFDM with parameters $N_t = N_r = S = L = M = 2$. Therefore, four streams are transmitted simultaneously. Assume that a and b are assigned to be the first and second streams transmitted by the first subcarrier respectively, and c and d are assigned to be the first and second streams transmitted by the second subcarrier respectively. The α-spectra can be figured out from the transfer function. For example, there are two error events with $d_h = 5$ whose α-spectra are $[2\,2;\;0\,1]$ and $[0\,1;\;2\,2]$ respectively.

This method can be applied to any $\mathcal{K}$-state k_c/n_c-rate convolutional code and BICMB-OFDM with M subcarriers and S streams transmitted at each subcarrier. If the spatial de-multiplexer is not a random switch for the whole packet, the period of the spatial de-multiplexer is an integer multiple of the Least Common Multiple (LCM) of n_c and SM. Note that a period of the interleaver is restricted to correspond to an integer multiple of trellis sections. Define $P = LCM(n_c, SM)$ as the number of coded bits for a minimum period. Then, the dimension of the vector $\mathbf{x}$ is $nP(\mathcal{K}-1)k_c/n_c$ where n is the integer multiple for a period of interest.

B. Full Diversity Condition

Based on the results of (20) and (21), full diversity of N_rN_tL [3] can be achieved if and only if all elements in the first column of the $\mathbf{A}$ matrix are non-zero, i.e., $\alpha_{m,1} \neq 0, \forall m$, for all error events. To meet such requirements of the α-spectra, the condition $R_cSL \leq 1$ needs to be satisfied. In the following, the proof of the full diversity condition with the rate of the convolutional code is provided.

Proof: To prove the necessity, assume that an information bit sequence $\mathbf{b}$ with length JR_cSL is transmitted, then a bit sequence $\mathbf{c}_{m,s}$ containing J bits is transmitted at the sth subchannel of the mth subcarrier. If $R_cSL > 1$, because the number of different codewords 2^{JR_cSL} is larger than the number of different bit sequences $\mathbf{c}_{m,s}$, 2^J, there always exists a pair of codewords result in the same $\mathbf{c}_{m,s}$. As a result, the pairs of codewords with the same $\mathbf{c}_{m,1}$ cause full diversity loss.

To prove the sufficiency, consider a bit interleaver employing simple rotation with the condition $R_c S L \leq 1$. In this case, all subchannels at each subcarrier could be assigned to one branch of the trellis structure of the convolutional code. Since the trellis of the convolutional can be designed such that the coded bits generated from the first branch splitting from the zero state are all error bits of an error event, each subchannel of all subcarriers could be used at least once for all error paths, which guarantees $\alpha_{m,1} \neq 0, \forall m$. Therefore, full diversity can be achieved.

This concludes the proof. □

The proof of the necessity above implies that in the case of $R_c S L > 1$, there always exists an error path with no error bits transmitted through the first subchannel of a subcarrier. Therefore, full diversity cannot be achieved. In this case, the bit interleaver should be designed such that consecutive coded bits are transmitted over different subchannels of different subcarriers to provide the maximum achievable diversity, which depends on the α-spectra.

V. NEGATIVE EFFECT OF SUBCARRIER CORRELATION

In practice, M is always much larger than L. In this case, correlation exists among subcarriers as shown in (17) and [32]. Hence, to calculate (15), the joint Probability Density Function (PDF) of $\mathbf{\Lambda}(m)\mathbf{\Lambda}^H(m)$ for all m satisfying $\mathbf{a}_m \neq \mathbf{0}$, which are eigenvalues of a set of correlated Wishart matrices [31], is required. However, this is an extremely difficult problem. The PDF of eigenvalues of two correlated Wishart matrices are given in [33], [34], [35], which is already highly complicated. To the best of our knowledge, the joint PDF of eigenvalues of more than two correlated Wishart matrices is not available in the literature. The maximum diversity of an OFDM-MIMO system is known to be $N_r N_t L$ [3]. In our case, however, a performance degradation caused by correlation is to be expected. Because, otherwise, the diversity can exceed the full diversity of $N_r N_t L$, which is a contradiction. In this section, the negative effect of correlation on the performance between two subcarriers is investigated to provide an intuitive insight.

Consider an error path whose d_H distinct bits between the bit codewords are all transmitted through two correlated subcarriers with correlation ρ, which could be the practical case. Define $X = \max(N_t, N_r)$ and $Y = \min(N_t, N_r)$. Let $\mathbf{\Phi} = [\phi_1, \ldots, \phi_Y]$ and $\tilde{\mathbf{\Phi}} = [\tilde{\phi}_1, \ldots, \tilde{\phi}_Y]$ denote the ordered eigenvalues of the two correlated Wishart matrices $\mathbf{H}\mathbf{H}^H$ and $\tilde{\mathbf{H}}\tilde{\mathbf{H}}^H$, respectively. Note that $\phi_u = \lambda_u^2$ in (15). Let $\mathbf{a} = [\alpha_1, \ldots, \alpha_Y]$ and $\tilde{\mathbf{a}} = [\tilde{\alpha}_1, \ldots, \tilde{\alpha}_Y]$ denote the α-spectra of $\mathbf{\Phi}$ and $\tilde{\mathbf{\Phi}}$ respectively. Define $\mathbf{p} = [p_1, \ldots, p_W]$

and $\tilde{\mathbf{p}} = [\tilde{p}_1, \ldots, \tilde{p}_{\tilde{W}}]$ whose elements are the indices corresponding to non-zero elements in $\mathbf{a}$ and $\tilde{\mathbf{a}}$, respectively, i.e, $\alpha_{p_w} \neq 0$ and $\alpha_{\tilde{p}_{\tilde{w}}} \neq 0$. Similarly, define $\mathbf{q} = [q_1, \ldots, q_{Y-W}]$ and $\tilde{\mathbf{q}} = [\tilde{q}_1, \ldots, \tilde{q}_{Y-\tilde{W}}]$ whose elements are the indices corresponding to zero elements in $\mathbf{a}$ and $\tilde{\mathbf{a}}$, respectively, i.e, $\alpha_{q_w} = 0$ and $\alpha_{\tilde{q}_{\tilde{w}}} = 0$. Define $\mathbf{\Phi_p} = [\phi_{p_1}, \ldots, \phi_{p_w}]$, $\tilde{\mathbf{\Phi}}_{\tilde{\mathbf{p}}} = [\tilde{\phi}_{\tilde{p}_1}, \ldots, \tilde{\phi}_{\tilde{p}_{\tilde{w}}}]$, $\mathbf{\Phi_q} = [\phi_{q_1}, \ldots, \phi_{q_w}]$, and $\tilde{\mathbf{\Phi}}_{\tilde{\mathbf{q}}} = [\tilde{\phi}_{\tilde{q}_1}, \ldots, \tilde{\phi}_{\tilde{q}_{\tilde{w}}}]$. Therefore, the PEP in (15) is written as

$$\begin{aligned}\Pr\left(\mathbf{c} \to \hat{\mathbf{c}}\right) &\leq \mathrm{E}\left\{\exp\left[-\frac{d_{min}^2\left(\mathbf{a}^T\mathbf{\Phi} + \tilde{\mathbf{a}}^T\tilde{\mathbf{\Phi}}\right)}{4N_0}\right]\right\} \\ &\leq \mathrm{E}\left\{\exp\left[-\mu\left(\sum_{w=1}^{W}\phi_{p_w} + \sum_{\tilde{w}=1}^{\tilde{W}}\tilde{\phi}_{\tilde{p}_{\tilde{w}}}\right)\right]\right\} \end{aligned} \tag{25}$$

with $\mu = \left(d_{min}^2\alpha_{min}\right) / \left(4N_0\right)$, where α_{min} indicates the minimum element in $\mathbf{a}$ and $\tilde{\mathbf{a}}$. To solve (25), the marginal PDF $f(\mathbf{\Phi_p}, \tilde{\mathbf{\Phi}}_{\tilde{\mathbf{p}}})$ is needed by calculating

$$f(\mathbf{\Phi_p}, \tilde{\mathbf{\Phi}}_{\tilde{\mathbf{p}}}) = \int\cdots\int_{\mathcal{D}_{\mathbf{q}}}\int\cdots\int_{\mathcal{D}_{\tilde{\mathbf{q}}}} f(\mathbf{\Phi}, \tilde{\mathbf{\Phi}})\,\mathrm{d}\mathbf{\Phi_q}\,\mathrm{d}\tilde{\mathbf{\Phi}}_{\tilde{\mathbf{q}}}. \tag{26}$$

The joint PDF $f(\mathbf{\Phi}, \tilde{\mathbf{\Phi}})$ is available in [33], [34], as

$$f(\mathbf{\Phi}, \tilde{\mathbf{\Phi}}) = \exp\left[-\frac{1}{1-\rho^2}\sum_{u=1}^{Y}\left(\phi_u + \tilde{\phi}_u\right)\right] f_1(\mathbf{\Phi}, \tilde{\mathbf{\Phi}}), \tag{27}$$

with the polynomial $f_1(\mathbf{\Phi}, \tilde{\mathbf{\Phi}})$ defined as

$$f_1(\mathbf{\Phi}, \tilde{\mathbf{\Phi}}) = [\prod_{u<v}^{Y}(\phi_u - \phi_v)(\tilde{\phi}_u - \tilde{\phi}_v)] \times |(\phi_u\tilde{\phi}_v)^{(X-Y)/2} I_{X-Y}(2\sqrt{\epsilon\phi_u\tilde{\phi}_v})|, \tag{28}$$

where $|H_{u,v}|$ represents the determinant of the matrix with the (u, v)th element given by $H_{u,v}$, $I_u(\cdot)$ is a modified Bessel function of order u which is given by

$$I_N(t) = \sum_{j=0}^{\infty}\frac{1}{j!(j+N+1)!}\left(\frac{t}{2}\right)^{2j+N}, \tag{29}$$

and $\epsilon \approx \rho^2/(1-\rho^2)^2$. Because the exponent of μ is related to the diversity, the constant appearing in the literature is ignored in (28) for brevity.

Since the eigenvalues of the Wishart matrices are positive and real, $\exp(\frac{1}{1-\rho^2}\phi_u) \leq 1$ and $\exp(\frac{1}{1-\rho^2}\tilde{\phi}_u) \leq 1$ in (27). By applying $\int_0^v u^t e^{-u}\,\mathrm{d}u \leq \frac{1}{t+1}v^{t+1}$ and $\int_0^\infty u^t e^{-u}\,\mathrm{d}u = t!$ to $\mathbf{\Phi_q}$ and $\tilde{\mathbf{\Phi}}_{\tilde{\mathbf{q}}}$, the marginal PDF

$f(\mathbf{\Phi_p}\tilde{\mathbf{\Phi}}_{\tilde{\mathbf{p}}})$ in (26) is upper bounded as

$$f(\mathbf{\Phi_p}, \tilde{\mathbf{\Phi}}_{\tilde{\mathbf{p}}}) \leq \exp\left[-\frac{\left(\sum_{w=1}^{W}\phi_{p_w} + \sum_{\tilde{w}=1}^{\tilde{W}}\tilde{\phi}_{\tilde{p}_{\tilde{w}}}\right)}{1-\rho^2}\right] \times f_2(\mathbf{\Phi_p}, \tilde{\mathbf{\Phi}}_{\tilde{\mathbf{p}}}), \tag{30}$$

where $f_2(\mathbf{\Phi_p}, \tilde{\mathbf{\Phi}}_{\tilde{\mathbf{p}}})$ is a polynomial corresponding to (27). Then (25) is rewritten as

$$\begin{aligned}\Pr\left(\mathbf{c} \to \hat{\mathbf{c}}\right) \leq & \int_0^{\infty}\int_0^{\phi_{p_1}}\cdots\int_0^{\phi_{p_{W-1}}}\int_0^{\infty}\int_0^{\phi_{\tilde{p}_1}}\cdots\int_0^{\phi_{\tilde{p}_{\tilde{W}-1}}} \\ & \exp\left[-\left(\mu + \frac{1}{1-\rho^2}\right)\left(\sum_{w=1}^{W}\phi_{p_w} + \sum_{\tilde{w}=1}^{\tilde{W}}\tilde{\phi}_{\tilde{p}_{\tilde{w}}}\right)\right] \times f_2(\mathbf{\Phi_p}, \tilde{\mathbf{\Phi}}_{\tilde{\mathbf{p}}})\,\mathrm{d}\mathbf{\Phi_p}\,\mathrm{d}\tilde{\mathbf{\Phi}}_{\tilde{\mathbf{p}}}.\end{aligned} \tag{31}$$

Note that since $f_2(\mathbf{\Phi_p}, \tilde{\mathbf{\Phi}}_{\tilde{\mathbf{p}}})$ is a polynomial, its multivariate terms can be integrated separately, and the term with the worst performance dominates the overall performance. To solve (31), a theorem provided in [30] can be applied to integrate $\mathbf{\Phi_p}$ and $\tilde{\mathbf{\Phi}}_{\tilde{\mathbf{p}}}$ independently for each multivariate term, which is given below.

Theorem 2. *For a multivariate term with variable ϕ_w for $w = 1, \ldots, W$ whose exponent, denoted by β_w, is a non-negative integer, the multiple integration in a domain $\infty > \phi_1 > \cdots > \phi_W > 0$ is*

$$\int_0^{\infty}\int_0^{\phi_1}\cdots\int_0^{\phi_{W-1}}\sum_{w=1}^{W}\left(\phi_w^{\beta_w}e^{-\mu\phi_w}\right)\,\mathrm{d}\phi_W\cdots,\,\mathrm{d}\phi_1 = \zeta\mu^{-\left(W+\sum_{w=1}^{W}\beta_w\right)}, \tag{32}$$

where ζ is a constant.

Proof: See [30]. □

Based on Theorem 2, the multivariate term with the smallest degree in $f_2(\mathbf{\Phi_p}, \tilde{\mathbf{\Phi}}_{\tilde{\mathbf{p}}})$ results in the smallest degree of $(\mu + \frac{1}{1-\rho^2})^{-1}$, which dominates the overall performance. The smallest degree of $f_2(\mathbf{\Phi_p}, \tilde{\mathbf{\Phi}}_{\tilde{\mathbf{p}}})$ is $(X - p_1 + 1)(Y - p_1 + 1) + (X - \tilde{p}_1 + 1)(Y - \tilde{p}_1 + 1) - W - \tilde{W}$, and the proof is provided in Appendix A. Therefore, (31) is upper bounded by

$$\Pr\left(\mathbf{c} \to \hat{\mathbf{c}}\right) \leq \zeta\left(\frac{d_{min}^2\alpha_{min}}{4N_t}\gamma + \frac{1}{1-\rho^2}\right)^{-D}, \tag{33}$$

with $D = (X - p_1 + 1)(Y - p_1 + 1) + (X - \tilde{p}_1 + 1)(Y - \tilde{p}_1 + 1)$, where ζ is a constant.

The negative effect of subcarrier correlation is proved by (33). When $\gamma \to \infty$, the diversity is the same as the uncorrelated case. However, on the practical range, the performance is degraded due to the term $\frac{1}{1-\rho^2}$, which is independent of SNR. Specifically, when the subcarrier correlation ρ is small, $\frac{1}{1-\rho^2}$ is also relatively small, and its effect on the performance is not significant when the SNR is relatively large, and the uncorrelated case $\rho = 0$ offers the performance upper bound. On the other hand, when ρ is large, $\frac{1}{1-\rho^2}$ is also relatively large compared to the SNR, then significant performance degradation could be caused, depending on the SNR. When $\rho = 1$, which means all the distinct bits of the error path are transmitted through one subcarrier, no multipath diversity is achieved, and the diversity equals BICMB in the case of flat fading channels introduced in [10], [11], which provides the performance lower bound. Note that the analysis in this section is not limited to equal power channel taps, and can also be applied to unequal power channel taps, non-constant sampling time, and other assumptions, which cause different subcarrier correlation.

VI. SUBCARRIER GROUPING

The idea of subcarrier grouping technique is to transmit multiple streams of information through multiple group of subcarriers of OFDM. It was suggested for multi-user interference elimination [22], Peak-to-Average Ratio (PAR) reduction [23], and complexity reduction [24]. In this paper, the subcarrier correlation technique is applied to overcome the performance loss caused by subcarrier correlation.

Note that $\rho = 0$ in (17) when $(m - m')L/M \in \mathbb{Z}$, where $\mathbb{Z}$ denotes the set of integer numbers. This means that although correlation exists among subcarriers for $L < M$, some subcarriers could be uncorrelated if $M/L \in \mathbb{Z}$. In this case, there are M/L groups of L uncorrelated subcarriers. As a result, the subcarrier grouping technique is applied to transmit multiple streams of bit codewords through these M/L different groups of uncorrelated subcarriers, instead of transmitting one stream of the bit codeword through all the correlated subcarriers. As a result, the negative effect of subcarrier correlation is completely avoided, and the maximum achievable diversity is thereby achieved. For example, consider the case of $L = 2$ and $M = 64$. Then, the uth and the $(u + 32)$th subcarriers are uncorrelated for $u = 1, \ldots, 32$. The subcarrier grouping technique can transmit 32 streams of bit codewords simultaneously through the 32 groups of two uncorrelated subcarriers without performance degradation. Note that the best choice of the number of subcarriers in one group is L, since smaller choice results in less diversity while larger choice causes subcarrier correlation which degrades performance.

Fig. 5 presents the structure of BICMB-OFDM with subcarrier grouping. In Fig. 5, $\mathbf{T}_1$ is a permutation matrix at the transmitter distributing modulated scalar symbols from different streams to their corresponding subcarriers, while $\mathbf{T}_2 = \mathbf{T}_1^{-1}$ is a permutation matrix at the receiver distributing received scalar symbols of different subcarriers to their corresponding streams for decoding. Compared to BICMB-OFDM

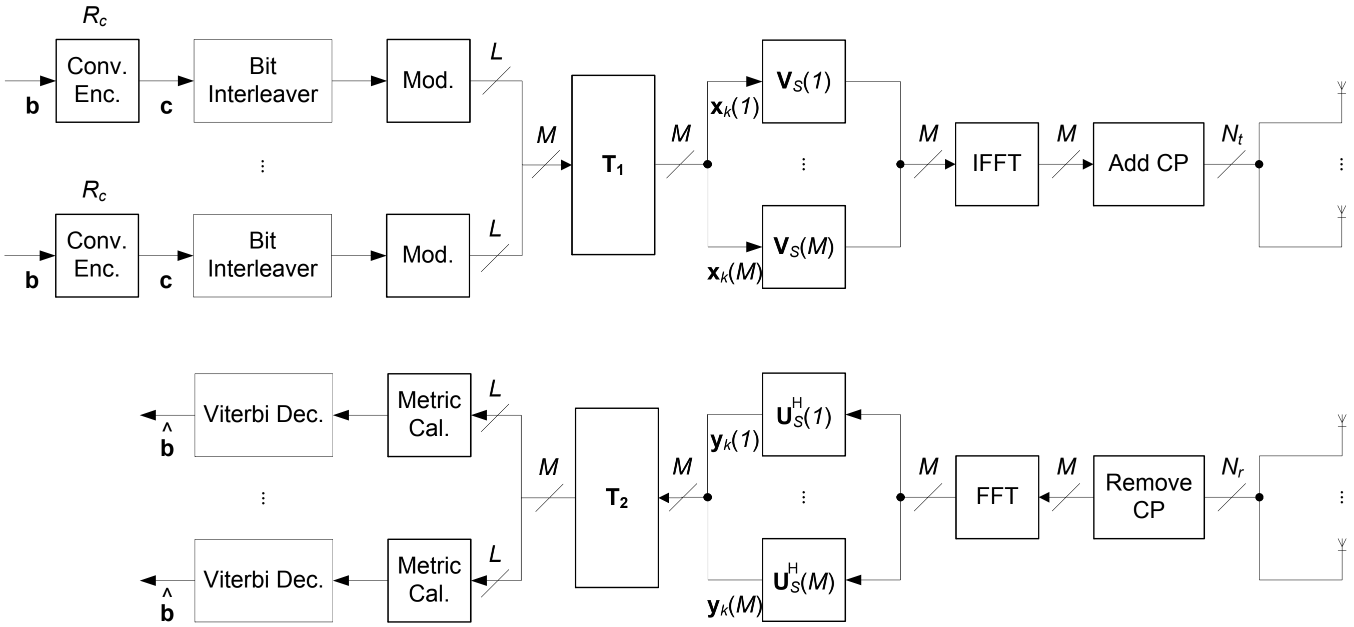

Fig. 5. Structure of BICMB-OFDM with subcarrier grouping.

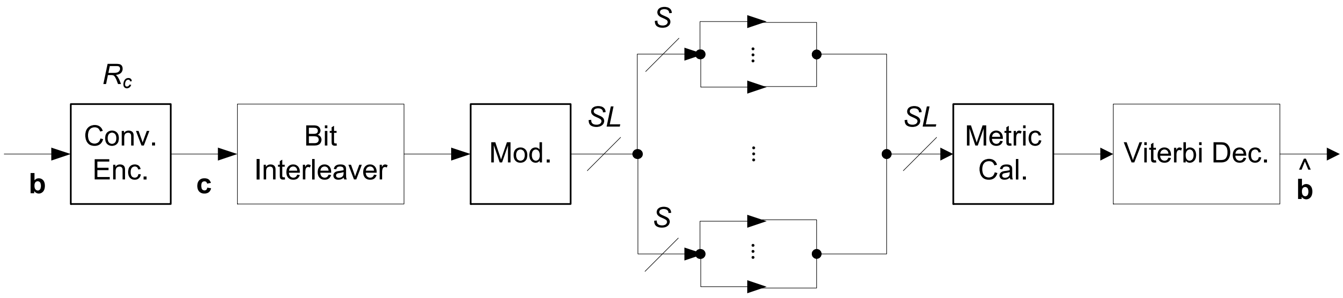

Fig. 6. Structure of BICMB-OFDM with subcarrier grouping in the frequency domain for one bit stream transmission.

without subcarrier grouping, BICMB-OFDM with subcarrier grouping achieves better performance with the same transmission rate and decoding complexity. Note that the structure of BICMB-OFDM with subcarrier grouping can also be considered as Orthogonal Frequency-Division Multiple Access (OFDMA) [15] version of BICMB-OFDM. OFDMA is a multi-user version of the OFDM and it has been used in the mobility mode of WiMax [17] as well as the downlink of LTE [18]. The multiple access in OFDMA is achieved by assigning subsets of subcarriers to individual users, which is similar to the subcarrier grouping technique. As a result, with subcarrier grouping, BICMB-OFDM can provide multi-user compatibility.

Fig. 6 presents the structure of BICMB-OFDM with subcarrier grouping in the frequency domain for one bit stream transmission. Note that Fig. 6 also presents the structure of BICMB-OFDM in the frequency domain when $L = M$. Therefore, the diversity analysis for $L = M$ in Section IV can be applied to BICMB-OFDM with subcarrier grouping. As a result, the full diversity condition $R_cSL \leq 1$ holds for

BICMB-OFDM with subcarrier grouping. In this paper, the number of employed subchannels by SVD for each subcarrier is assumed to be the same, which is S. However, they could be different in practice. In that case, the full diversity condition is $R_c \sum_{l=1}^{L} S_{u,l} \leq 1$ for $u = 1, \ldots, M/L$, where $S_{u,l}$ denotes the number of employed subchannels by SVD for the lth subcarrier of the uth group.

Note that (17) is derived under the assumption that all channel taps have the same power. When they have different power, there are no uncorrelated subcarriers in general. However, some of them could have weak correlation. Therefore, the subcarrier grouping can still be applied to combat the diversity degradation, although it now can no longer fully recover the maximum achievable diversity because of subcarrier correlation.

VII. SIMULATION RESULTS

To verify the diversity analysis, 2×2 $M = 64$ BICMB-OFDM with $L = 2$ and $L = 4$ using 4-QAM are considered for simulations. The number of employed subchannels for each subcarrier is assumed to be the same. The generator polynomials in octal for the convolutional codes with $R_c = 1/4$ and $R_c = 1/2$ are $(5, 7, 7, 7)$, and $(5, 7)$ respectively, and the codes with $R_c = 2/3$ and $R_c = 4/5$ are punctured from the $R_c = 1/2$ code [25]. The length of CP is $L_{CP} = 16$. Each OFDM symbol has $4\mu\text{s}$ duration, of which $0.8\mu\text{s}$ is CP. Equal and exponential power channel taps are considered. For the exponential channel model [36], the ratios of non-negligible path power to the first path power are -7dB, the mean excess delays are $30ns$ for $L = 2$ and $65ns$ for $L = 4$, respectively. The bit interleaver employs simple rotation. Note that simulations of 2×2 $L = 2$ and $L = 4$ BICMB-OFDM are shown in this section because the diversity values could be investigated explicitly through figures.

Fig. 7 shows the Bit Error Rate (BER) performance of 2×2 $L = 2$ $M = 64$ BICMB-OFDM employing subcarrier grouping over equal power channel taps with different S and R_c. The $\mathbf{A}$ matrices that dominate the performance are provided in the figure. The diversity results of all curves equals the maximum achievable diversity orders derived from Section IV, which is directly decided by the $\mathbf{A}$ matrices. Specifically, in the cases of $S = 1$, $R_c = 1/4$ and $R_c = 2/3$ codes, whose dominant $\mathbf{A}$ matrices are $\mathbf{A} = [2;\ 3]$ and $\mathbf{A} = [0;\ 5]$ respectively, achieve diversity values of 8 and 4 respectively. For $S = 2$, the codes with $R_c = 1/4$, $R_c = 1/2$, $R_c = 2/3$, and $R_c = 4/5$, whose dominant $\mathbf{A}$ matrices are $\mathbf{A} = [2\,3; 3\,3]$, $\mathbf{A} = [0\,1; 2\,2]$, $\mathbf{A} = [0\,0; 2\,2]$, and $\mathbf{A} = [0\,0; 0\,4]$ respectively, offer diversity of 8, 5, 2, and 1 respectively. Note that full diversity of 8 is achieved with the condition $R_c S L \leq 1$.

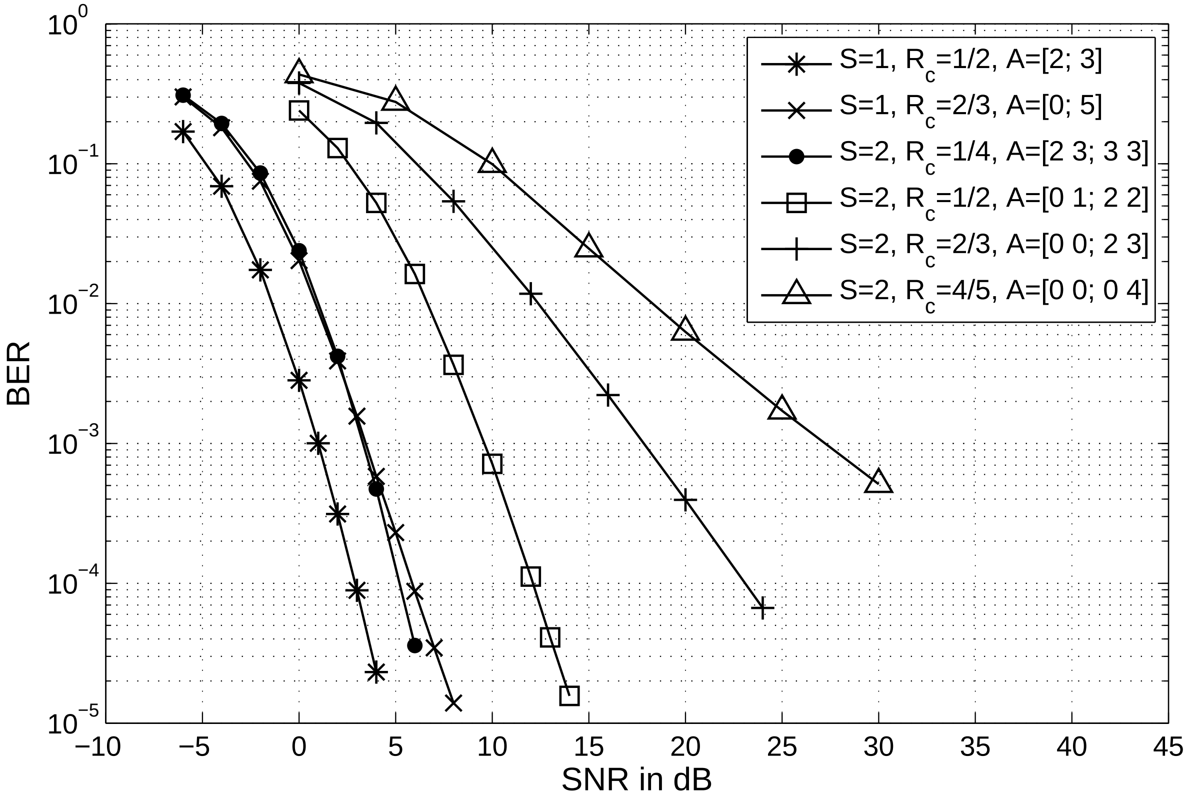

Fig. 7. BER vs. SNR for 2×2 $L = 2$ $M = 64$ BICMB-OFDM with subcarrier grouping over equal power channel taps.

Similarly, Fig. 8 shows the BER performance of 2×2 $L = 4$ $M = 64$ $S = 1$ BICMB-OFDM employing subcarrier grouping over equal power channel taps with different R_c. The $\mathbf{A}$ matrices that dominate the performance are provided in the figure. The diversity results of all curves equals the maximum achievable diversity orders derived from Section IV, which is directly decided by the $\mathbf{A}$ matrices. Specifically, the codes with $R_c = 1/4$, $R_c = 1/2$, $R_c = 2/3$, and $R_c = 4/5$, whose dominant $\mathbf{A}$ matrices are $\mathbf{A} = [2;\ 3;\ 3;\ 3]$, $\mathbf{A} = [0;\ 1;\ 2;\ 2]$, $\mathbf{A} = [0;\ 0;\ 2;\ 2]$, and $\mathbf{A} = [0;\ 0;\ 0;\ 4]$ respectively, offer diversity of 16, 12, 8, and 4 respectively. Note that full diversity of 16 is achieved with the condition $R_cSL \leq 1$.

Fig. 9 shows the BER performance of examined PEPs in (15) with $S = 2$, where the simplest case of an error event with $d_H = 2$ is examined for two subcarriers with different correlation coefficient ρ, which is derived from the 2×2 $L = 2$ $M = 64$ BICMB-OFDM over equal power channel taps. The figure shows that when $\rho = 0$, which implies the two subcarriers are uncorrelated, $\mathbf{A} = [1\,0; 1\,0]$ and $\mathbf{A} = [1\,0; 0\,1]$ offer diversity of 8 and 5 respectively. On the other hand, when $\rho \neq 0$, performance degradation is caused by subcarrier correlation, and stronger correlation results in worse performance loss. When $\rho = 1$, which means the $d_H = 2$ distinct bits are transmitted through only one subcarrier and no multipath diversity is

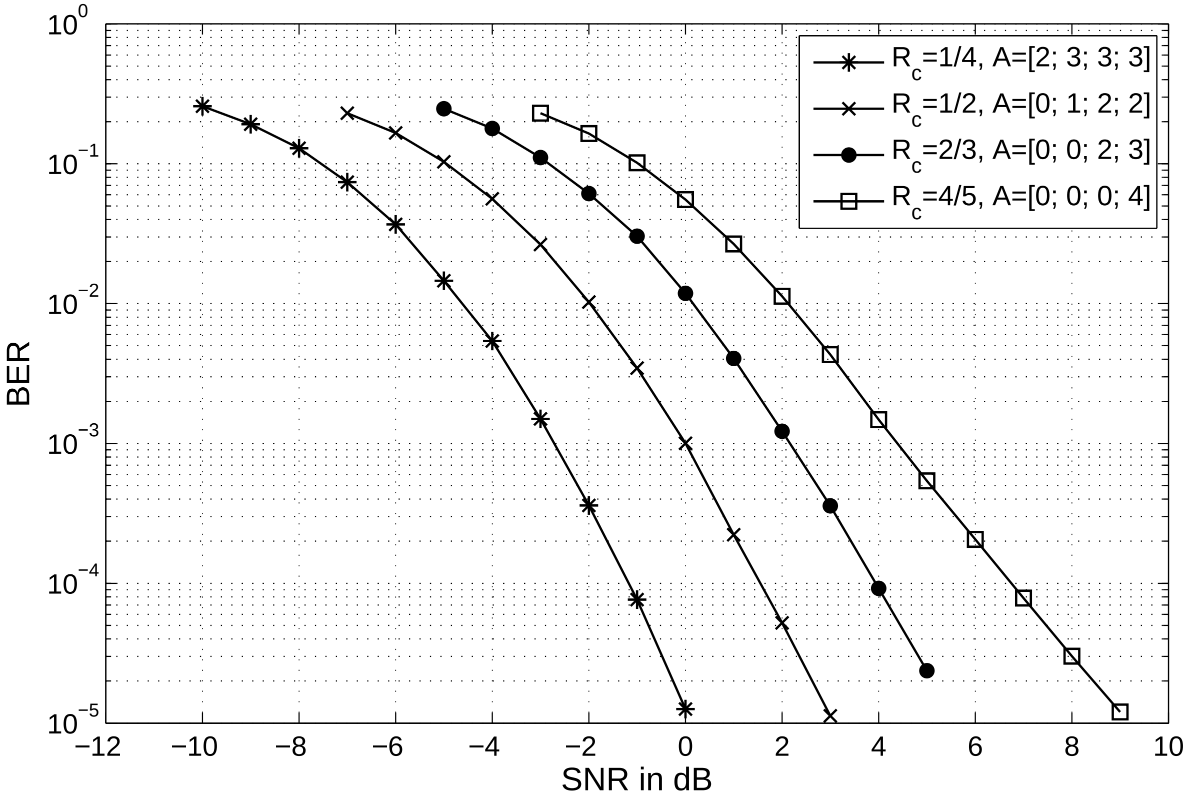

Fig. 8. BER vs. SNR for 2×2 $L = 4$ $M = 64$ $S = 1$ BICMB-OFDM with subcarrier grouping over equal power channel taps.

achieved, both $\mathbf{A} = [2\,0; 0\,0]$ and $\mathbf{A} = [1\,1; 0\,0]$ provide diversity of 4. The results are consistent with the analysis provided in Section V, and they show the negative effect of subcarrier correlation on performance.

Fig. 10 shows the BER performance of 2×2 $L = 2$ $M = 64$ $S = 1$ $R_c = 1/2$ BICMB-OFDM with and without subcarrier grouping over equal and exponential power channel taps. In the figure, w/ and w/o denote with and without respectively, while SG denotes subcarrier grouping. The results show that the subcarrier grouping technique can combat the performance loss caused by subcarrier correlation for both equal and exponential power channel taps. As discussed in Section VI, the maximum achievable diversity of 8 is provided by employing subcarrier grouping for equal power channel taps, since there is no subcarrier correlation. As for the case of exponential power channel taps, subcarrier grouping cannot fully recover the performance loss because subcarrier correlation still exists.

Fig. 11 shows the correlation ρ of two subcarriers with different separation for 2×2 $L = 2$ $M = 64$ BICMB-OFDM over equal and exponential power channel taps. The figure shows that the channel with exponential power taps causes stronger subcarrier correlation than equal power taps, which results in worse performance as shown in Fig. 10.

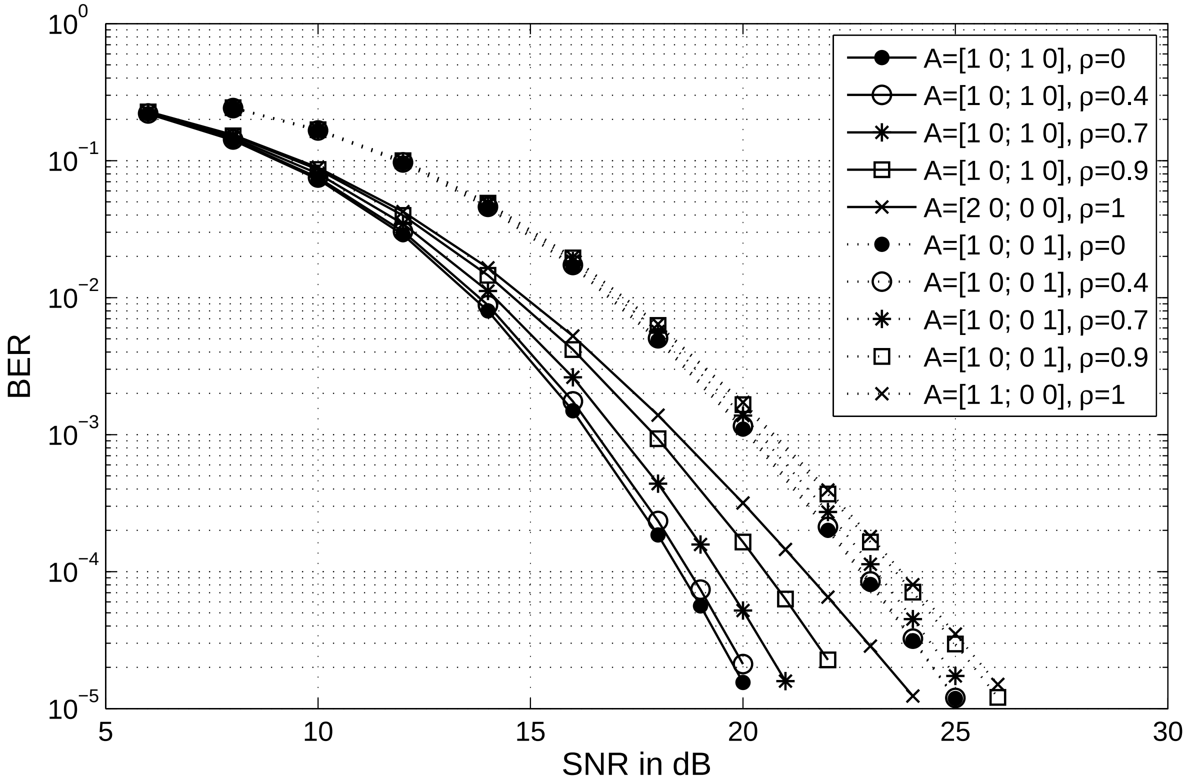

Fig. 9. BER vs. SNR for examined PEPs of two subcarriers with different correlation for 2×2 $L = 2$ $M = 64$ $S = 2$ BICMB-OFDM over equal power channel taps.

Similarly to Fig. 10, Fig. 12 shows the BER performance of 2×2 $L = 4$ $M = 64$ $S = 1$ $R_c = 1/4$ BICMB-OFDM with and without subcarrier grouping over equal and exponential power channel taps. The results show that the negative effect of subcarrier correlation on performance can be overcome by the subcarrier grouping technique for both equal and exponential power channel taps. For equal power channel taps, the maximum achievable diversity of 16 is achieved by applying subcarrier grouping as discussed in Section VI because subcarrier correlation is totally removed. On the other hand, since subcarrier correlation is not totally reduced in the case of exponential power channel taps, subcarrier grouping cannot fully restore the performance degradation.

Similarly to Fig. 11, Fig. 13 shows the correlation ρ of two subcarriers with different separation for 2×2 $L = 4$ $M = 64$ BICMB-OFDM over equal and exponential power channel taps. The figure shows that the subcarrier correlation of exponential power channel taps is larger than equal power channel taps so that it achieves worse performance as shown in Fig. 12.

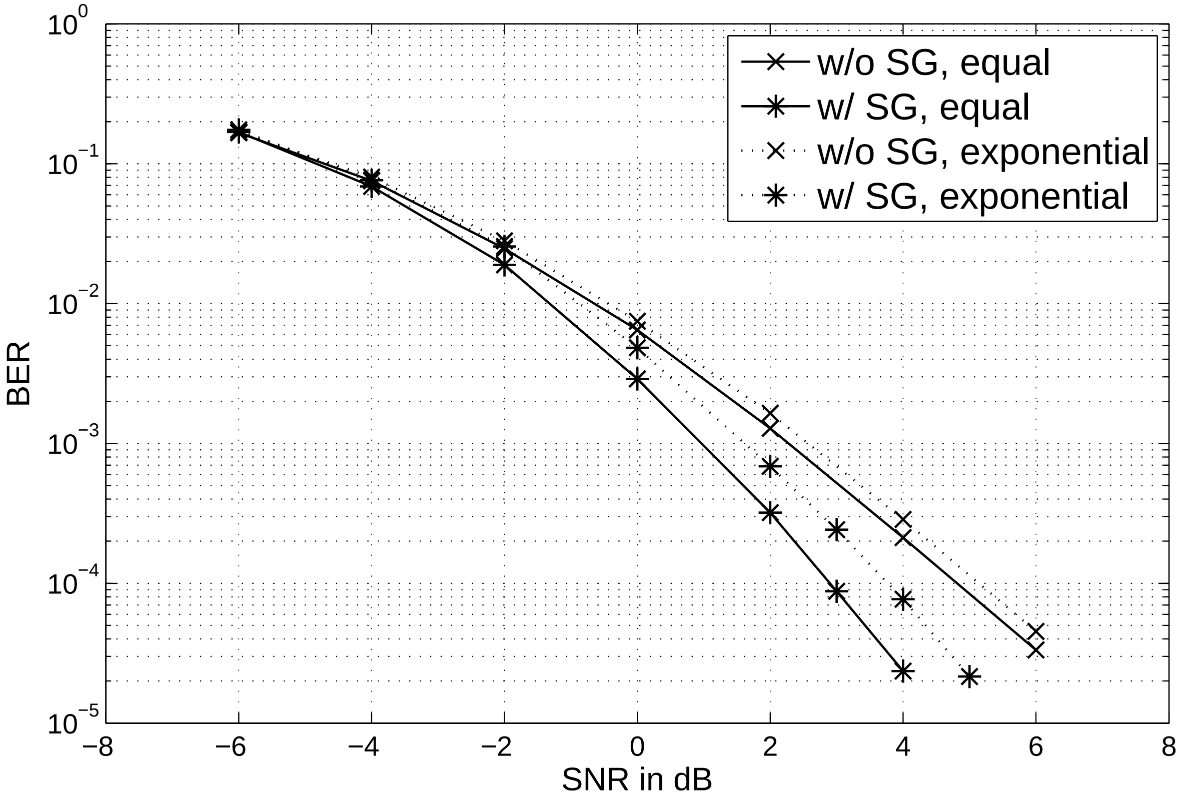

Fig. 10. BER vs. SNR for 2×2 $L = 2$ $M = 64$ $S = 1$ $R_c = 1/2$ BICMB-OFDM with and without subcarrier grouping over equal and exponential power channel taps.

A. Discussions

Fig. 9 verifies the negative effect of subcarrier correlation as analyzed in Section V, while Fig. 10 and Fig. 12 verify the advantage of BICMB-OFDM with subcarrier grouping over BICMB-OFDM without subcarrier grouping. Other than the subcarrier grouping technique, focus can be drawn on the design of the bit interleaver to combat the subcarrier correlation. As illustrated in Section IV-A, the bit interleaver is directly related to the α-spectra which reflect the subcarrier distribution of the distinct bits for each error path and thereby determine the diversity. In fact, the performance degradation results from the error paths whose distinct bits are transmitted by correlated subcarriers. Therefore, negative effect of subcarrier correlation can be reduced by a properly designed bit interleaver. However, such an interleaver only finds the better arrangement of subcarriers to lighten the negative effect of subcarrier correlation without actual reduction achieved by subcarrier grouping. As a result, the subcarrier grouping technique is apparently a better choice because it does not only achieve better performance but also provides multi-user compatibility as explained in Section VI. Therefore, the design of the bit interleaver to combat subcarrier correlation

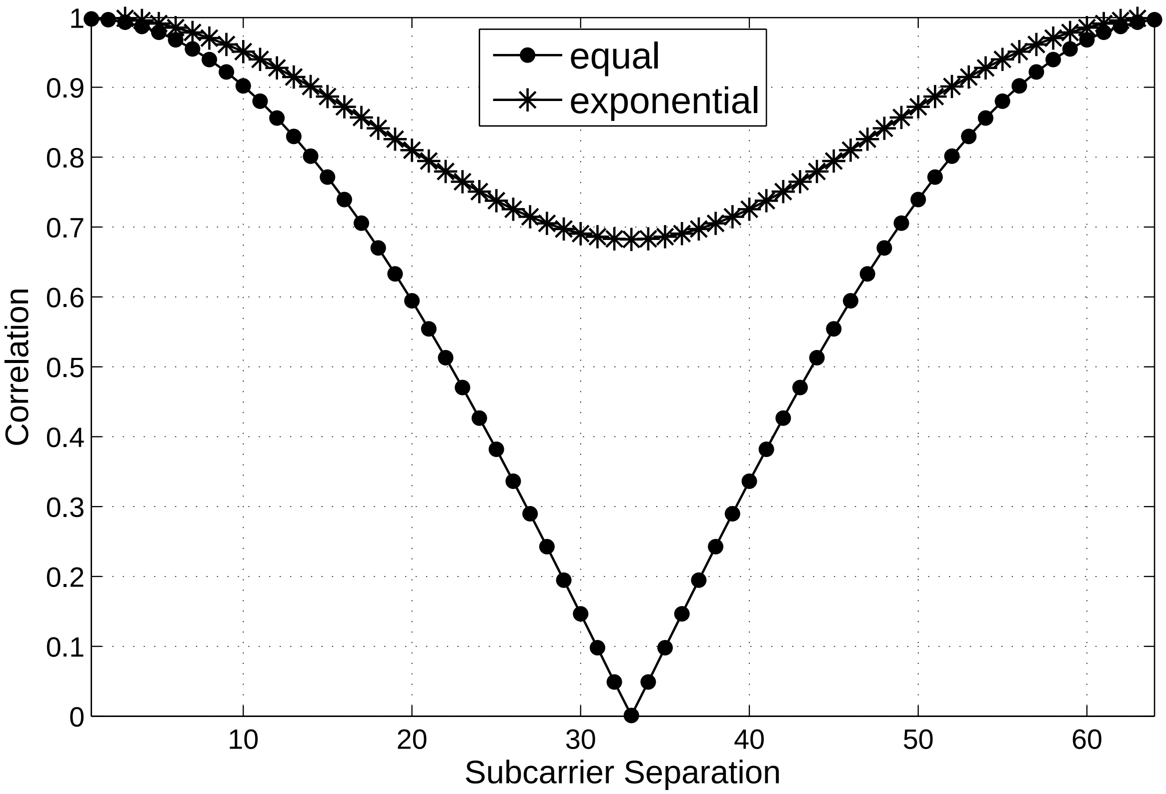

Fig. 11. Correlation vs. subcarrier separation for 2×2 $L = 2$ $M = 64$ BICMB-OFDM over equal and exponential power channel taps.

is not considered in this paper.

In this paper, FFT-based OFDM is considered in which CP is added to combat ISI. However, adding CP results in data rate loss. In order to avoid the extra CP data that reduce bandwidth, Discrete Wavelet Transform (DWT) and Inverse DWT (IDWT) has been considered as alternative platforms for OFDM to replace IFFT and FFT [37], [38], [39]. DWT-based OFDM is overall the same as FFT-based OFDM, and the only difference is in the OFDM modulator and demodulator. The DWT-based OFDM employs Low Pass Filter (LPF) and High Pass Filter (HPF) operating as quadrature mirror filters satisfying perfect reconstruction and orthonormal bases properties. The transform uses filter coefficients as approximate and detail in LPF and HPF respectively. The main advantage of DWT-based OFDM is that it does not need adding CP to combat ISI, and thereby provides higher data rate than FFT-based OFDM. However, the DWT-based OFDM requires more complicated equalization [40], [41], [42], than the simple frequency-domain single-tap equalization of FFT-based OFDM for frequency selective MIMO channels. As a result, the corresponding quasi-static flat fading MIMO channel for each frequency subcarrier in (10) may not be valid so that the SVD beamforming cannot be employed. Therefore, the FFT-based BICMB-OFDM

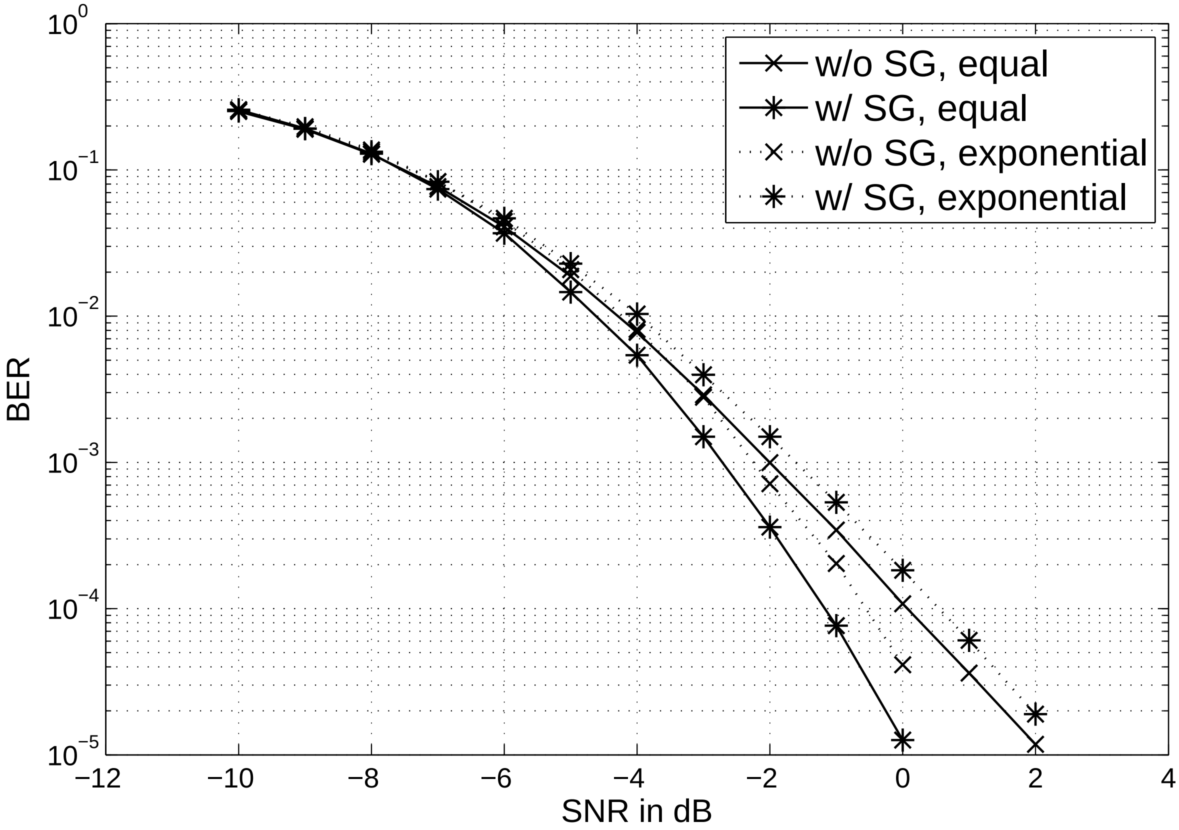

Fig. 12. BER vs. SNR for 2×2 $L = 4$ $M = 64$ $S = 1$ $R_c = 1/4$ BICMB-OFDM with and without subcarrier grouping over equal and exponential power channel taps.

proposed in this paper may not be applied to DWT-based OFDM. Nevertheless, if a single-tap equalization similar to (9) becomes available for DWT-based OFDM, then the BICMB-OFDM technique and its diversity analysis proposed in this paper become valid. The only difference is the subcarrier correlation so that a different selection needs to be considered for subcarrier grouping. The discussion on the existence of single-tap equalization technique for DWT-based OFDM is beyond the scope of this paper, so it is left for future considerations.

Fig. 7 and Fig. 8 verify the relation between the diversity and the α-spectra as well as the full diversity condition $R_cSL \leq 1$ derived in Section IV for BICMB-OFDM with subcarrier grouping. The full diversity condition implies that if the number of streams S transmitted at each subcarrier increases, the code rate R_c may have to decrease in order to keep full diversity. As a result, increasing the number of parallel streams may not fully improve the total transmission rate, which is a similar issue to the full diversity condition $R_cS \leq 1$ of BICMB for flat fading MIMO channels introduced in [10], [11]. In fact, for flat fading MIMO channels, other than channel coding, the constellation precoding technique has been incorporated with both

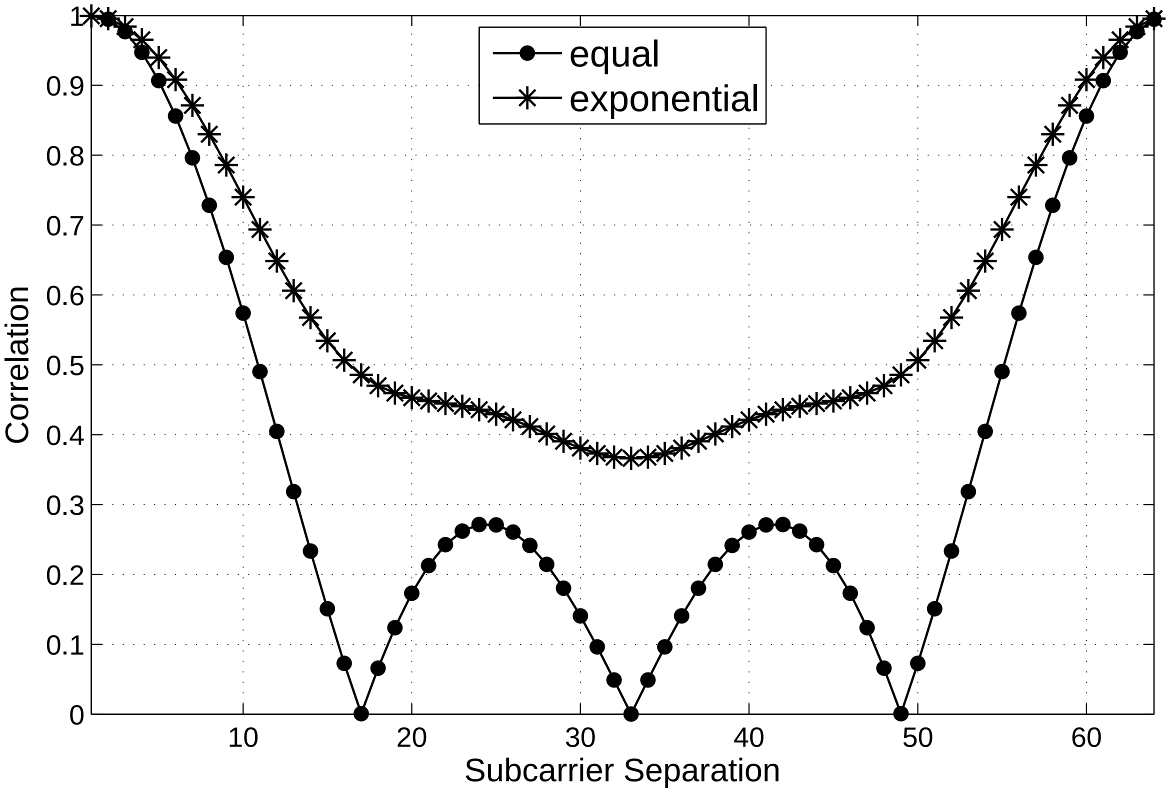

Fig. 13. Correlation vs. subcarrier separation for 2×2 $L = 4$ $M = 64$ BICMB-OFDM over equal and exponential power channel taps.

uncoded and coded SVD beamforming to achieve full diversity and full multiplexing simultaneously, with the trade-off of a higher decoding complexity [43], [44], [45], [46]. Specifically, in the uncoded case, full diversity requires that all streams are precoded. On the other hand, for the coded case, which is BICMB, even without the condition $R_c S \leq 1$, other than full precoding, partial precoding with lower decoding complexity than full precoding could also achieve both full diversity and full multiplexing with the properly designed combination of the convolutional code, the bit interleaver, and the constellation precoder. Moreover, Perfect Space-Time Block Codes (PSTBCs) [47], which have the properties of full rate, full diversity, uniform average transmitted energy per antenna, good shaping of the constellation, and nonvanishing constant minimum determinant for increasing spectral efficiency which offers high coding gain, have been considered as an alternative scheme to replace the constellation precoding technique for both uncoded and coded SVD beamforming with constellation precoding in order to reduce the decoding complexity in dimensions 2 and 4 while achieve almost the same performance [48], [49], [50]. Since these techniques have been successfully solved the restricted full diversity condition issue of $R_c S \leq 1$ for BICMB in the case of flat fading MIMO channels, it may be possible to incorporate these techniques with BICMB-OFDM so that its full diversity condition is not restricted to $R_c SL \leq 1$ for frequency selective MIMO channels. However, the design criteria and diversity analysis cannot be generalized in a straightforward manner because of the increased system complexity so that they are considered as future work.

VIII. CONCLUSIONS

BICMB-OFDM combines MIMO and OFDM to achieve both spatial diversity and multipath diversity for frequency selective MIMO channels so that it can be an important technique for broadband wireless communication. In this paper, the diversity analysis of BICMB-OFDM is carried out. As a result, the maximum achievable diversity is derived and the important α-spectra directly determining the diversity is introduced, providing important insights of BICMB-OFDM. According to the analysis, a sufficient and necessary condition $R_c SL \leq 1$ for achieving full diversity is proved, which is very important for practical design. In addition, the negative effect of subcarrier correlation on the performance in the practical case is investigated, and subcarrier grouping is employed to overcome the performance degradation and provide multi-user compatibility. Furthermore, it may be possible to employ precoding techniques so that the full diversity condition of BICMB-OFDM is not restricted to $R_c SL \leq 1$, and its diversity analysis and design criteria are considered as future work.

APPENDIX A

PROOF OF THE SMALLEST DEGREE OF $f_2(\mathbf{\Phi}_{\mathbf{p}}, \tilde{\mathbf{\Phi}}_{\tilde{\mathbf{p}}})$

The polynomial $f_2(\mathbf{\Phi}_{\mathbf{p}}, \tilde{\mathbf{\Phi}}_{\tilde{\mathbf{p}}})$ in (30) corresponds to (27). Because $\int_0^v u^t e^{-u} \, \mathrm{d}u \leq \frac{1}{t+1} v^{t+1}$ and $\int_0^\infty u^t e^{-u} \, \mathrm{d}u = t!$, the smallest degree of $f_2(\mathbf{\Phi}_{\mathbf{p}}, \tilde{\mathbf{\Phi}}_{\tilde{\mathbf{p}}})$ is related to the polynomial $f_1(\mathbf{\Phi}, \tilde{\mathbf{\Phi}})$ in (27), which is given by (28) and can be rewritten as

$$f_1(\mathbf{\Phi}, \tilde{\mathbf{\Phi}}) = \epsilon^{(X-Y)/2} [\prod_{u<v}^{Y} (\phi_u - \phi_v)(\tilde{\phi}_u - \tilde{\phi}_v)][\prod_{u=1}^{Y} (\phi_u \phi_v)^{X-Y}] |\tilde{I}_{X-Y}(\epsilon \phi_u \tilde{\phi}_v)|, \tag{34}$$

where

$$\tilde{I}_N(t) = \sum_{j=0}^{\infty} \frac{t^j}{j!(j+N+1)!}. \tag{35}$$

Note that only the multivariate term of $f_1(\mathbf{\Phi}, \tilde{\mathbf{\Phi}})$ determining the smallest degree of $f_2(\mathbf{\Phi}_{\mathbf{p}}, \tilde{\mathbf{\Phi}}_{\tilde{\mathbf{p}}})$ needs to be considered. The dominant term of $f_1(\mathbf{\Phi}, \tilde{\mathbf{\Phi}})$ is the one with the smallest degree and the largest eigenvalues, which depends on the dominant term of $\prod_{u<v}^{Y}(\phi_u-\phi_v)(\tilde{\phi}_u-\tilde{\phi}_v)$ and the dominant term of $|\tilde{I}_{X-Y}(\epsilon\phi_u\tilde{\phi}_v)|$. The dominant term of $\prod_{u<v}^{Y}(\phi_u-\phi_v)(\tilde{\phi}_u-\tilde{\phi}_v)$ is $\prod_{u=1}^{Y}(\phi_u\tilde{\phi}_u)^{Y-u}$. The dominant term of $|\tilde{I}_{X-Y}(\epsilon\phi_u\tilde{\phi}_v)|$ is $\zeta\prod_{u=1}^{Y}(\phi_u\tilde{\phi}_u)^{Y-u}$ where ζ is a constant, and the proof is provided in Appendix B. Therefore, the dominant term in $f_1(\mathbf{\Phi},\tilde{\mathbf{\Phi}})$ ignoring the constant, is given by

$$\tilde{f}_1(\mathbf{\Phi},\tilde{\mathbf{\Phi}})=\prod_{u=1}^{Y}(\phi_u\tilde{\phi}_u)^{X+Y-2u}. \tag{36}$$

The degree of $\tilde{f}_1(\mathbf{\Phi},\tilde{\mathbf{\Phi}})$ is

$$\delta_{\tilde{f}_1}=2[Y(Y-1)+Y(X-u)]. \tag{37}$$

After integration of (26), the factor $\prod_{u=1}^{p_1-1}\phi_u^{X+Y-2u}$ and the factor $\prod_{u=1}^{\tilde{p}_1-1}\tilde{\phi}_u^{X+Y-2u}$ of $\tilde{f}_1(\mathbf{\Phi},\tilde{\mathbf{\Phi}})$ vanish because $\int_0^\infty u^t e^{-u}\,\mathrm{d}u=t!$. Therefore,

$$\delta_{vanished}=(p_1-1)(X+Y-p_1)+(\tilde{p}_1-1)(X+Y-\tilde{p}_1). \tag{38}$$

Meanwhile, the eigenvalues ϕ_{q_u} with $q_u>p_1$ and $\phi_{\tilde{q}_u}$ with $\tilde{q}_u>\tilde{p}_1$ result in increased degree because $\int_0^v u^t e^{-u}\,\mathrm{d}u\le\frac{1}{t+1}v^{t+1}$. Therefore,

$$\delta_{added}=2Y-W-\tilde{W}-p_1-\tilde{p}_1+2. \tag{39}$$

As a result, the smallest degree of $f_2(\mathbf{\Phi}_{\mathbf{p}},\tilde{\mathbf{\Phi}}_{\tilde{\mathbf{p}}})$ is

$$\begin{aligned}\delta&=\delta_{\tilde{f}_1}-\delta_{vanished}+\delta_{added}\\&=(X-p_1+1)(Y-p_1+1)+(X-\tilde{p}_1+1)(Y-\tilde{p}_1+1)-W-\tilde{W}.\end{aligned} \tag{40}$$

APPENDIX B

PROOF OF THE DOMINANT TERM OF $|\tilde{I}_{X-Y}(\epsilon\phi_u\tilde{\phi}_v)|$

When $Y=1$,

$$|\tilde{I}_{X-Y}(\epsilon\phi_u\tilde{\phi}_v)|=\sum_{j=0}^{\infty}\frac{(\epsilon\phi_1\tilde{\phi}_1)^j}{j!(j+X)!} \tag{41}$$

and the dominant term is $1/X!$.

When $Y = 2$,

$$\begin{aligned}
|\tilde{I}_{X-Y}(\epsilon\phi_u\tilde{\phi}_v)| &= \tilde{I}_{X-Y}(\epsilon\phi_1\tilde{\phi}_1)\tilde{I}_{X-Y}(\epsilon\phi_2\tilde{\phi}_2) - \tilde{I}_{X-Y}(\epsilon\phi_1\tilde{\phi}_2)\tilde{I}_{X-Y}(\epsilon\phi_2\tilde{\phi}_1) \\
&= \sum_{j=0}^{\infty}\frac{(\epsilon\phi_1\tilde{\phi}_1)^j}{j!(j+X-1)!}\sum_{j=0}^{\infty}\frac{(\epsilon\phi_2\tilde{\phi}_2)^j}{j!(j+X-1)!} - \sum_{j=0}^{\infty}\frac{(\epsilon\phi_1\tilde{\phi}_2)^j}{j!(j+X-1)!}\sum_{j=0}^{\infty}\frac{(\epsilon\phi_2\tilde{\phi}_1)^j}{j!(j+X-1)!} \\
&= \sum_{u=1}^{2}\sum_{v=1}^{2}(-1)^{u+v}\left[\sum_{j=0}^{\infty}\sum_{k>j}^{\infty}\frac{(\epsilon\phi_u\tilde{\phi}_v)^j}{j!(j+X-1)!}\frac{(\epsilon\phi_{3-u}\tilde{\phi}_{3-v})^k}{k!(k+X-1)!}\right]
\end{aligned} \tag{42}$$

and the dominant term is $\epsilon\phi_1\tilde{\phi}_1/\left[X!(X-1)!\right]$.

When $Y \geq 3$,

$$|\tilde{I}_{X-Y}(\epsilon\phi_u\tilde{\phi}_v)| = \sum_{u=1}^{Y}\sum_{v=1}^{Y}(-1)^{u+v}\left[\prod_{k=1}^{Y}\sum_{j_k=0}^{\infty}\frac{(\epsilon\phi_{u_k}\tilde{\phi}_{v_k})^{j_k}}{j_k!(j_k+X-Y+1)!}\right]_{j_k<j_{k+1}} \tag{43}$$

where $u_k = [(u+k-2) \bmod Y] + 1$ and $v_k = [(v+k-2) \bmod Y] + 1$, and the dominant term is $\zeta\prod_{k=1}^{Y}(\phi_k\tilde{\phi}_k)^{Y-k}$ with $\zeta = \prod_{k=1}^{Y}\epsilon^{Y-k}/\left[(Y-k)!(X-k+1)!\right]$.

REFERENCES

[1] A. Paulraj, R. Nabar, and D. Gore, *Introduction to Space-Time Wireless Communication*. Cambridge University Press, 2003.

[2] L. Zheng. and D. Tse, “Diversity and Multiplexing: a Fundamental Tradeoff In Multiple-antenna Channels,” *IEEE Trans. Inf. Theory*, vol. 49, no. 5, pp. 1073–1096, May 2003.

[3] H. Jafarkhani, *Space-Time Coding: Theory and Practice*. Cambridge University Press, 2005.

[4] E. Sengul, E. Akay, and E. Ayanoglu, “Diversity Analysis of Single and Multiple Beamforming,” *IEEE Trans. Commun.*, vol. 54, no. 6, pp. 990–993, Jun. 2006.

[5] L. G. Ordoez, D. P. Palomar, A. Pages-Zamora, and J. R. Fonollosa, “High-SNR Analytical Performance of Spatial Multiplexing MIMO Systems with CSI,” *IEEE Trans. Signal Process.*, vol. 55, no. 11, pp. 5447–5463, Nov. 2007.

[6] E. Akay, E. Sengul, and E. Ayanoglu, “Achieving Full Spatial Multiplexing and Full Diversity in Wireless Communications,” in *Proc. IEEE WCNC 2006*, Las Vegas, NV, USA, Apr. 2006, pp. 2046–2050.

[7] ——, “Bit-Interleaved Coded Multiple Beamforming,” *IEEE Trans. Commun.*, vol. 55, no. 9, pp. 1802–1811, Sep. 2007.

[8] E. Akay, H. J. Park, and E. Ayanoglu. (2008) On ”Bit-Interleaved Coded Multiple Beamforming”. arXiv: 0807.2464. [Online]. Available: http://arxiv.org

[9] S. Lin and D. J. Costello, *Error Control Coding: Fundamentals and Applications*, 2nd ed. Prentice Hall,, 2004.

[10] H. J. Park and E. Ayanoglu, “Diversity Analysis of Bit-Interleaved Coded Multiple Beamforming,” in *Proc. IEEE ICC 2009*, Dresden, Germany, Jun. 2009.

[11] ——, “Diversity Analysis of Bit-Interleaved Coded Multiple Beamforming,” *IEEE Trans. Commun.*, vol. 58, no. 8, pp. 2457–2463, Aug. 2010.

[12] J. R. Barry, E. A. Lee, and D. G. Messerschmitt, *Digital Communication*, 3rd ed. Kluwer Academic Publishers, 2003.

[13] E. Akay and E. Ayanoglu, “Full Frequency Diversity Codes for Single Input Single Output Systems,” in *Proc. IEEE VTC 2004-Fall*, vol. 3, Los Angeles, CA, USA, Sep. 2004, pp. 1870–1874.

[14] ——, “Achieving Full Frequency and Space Diversity in Wireless Systems via BICM, OFDM, STBC, and Viterbi Decoding,” *IEEE Trans. Commun.*, vol. 54, no. 12, pp. 2164–2172, Dec. 2006.

[15] A. Ghosh, J. Zhang, J. G. Andrews, and R. Muhamed, *Fundamentals of LTE*. Prentice Hall, 2010.

[16] *IEEE Standard for Information Technology–Telecommunications and Information Exchange between Systems Local and Metropolitan Area Networks–Specific Requirements Part 11: Wireless LAN Medium Access Control (MAC) and Physical Layer (PHY) Specifications*, IEEE Std. 802.11-2012, Mar. 2012.

[17] *IEEE Approved Draft Standard for Local and Metropolitan Area Networks Part 16: Air Interface for Broadband Wireless Access Systems*, IEEE Std. 802.16-2012, Jun. 2012.

[18] *Evolved Universal Terrestrial Radio Access (E-UTRA); LTE physical layer; General description (Release 10)*, 3GPP Technical Specification 36.201 v10.0.0, Dec. 2010.

[19] H. Zamiri-Jafarian and M. Rajabzadeh, “A Polynomial Matrix SVD Approach for Time Domain Broadband Beamforming in MIMO-OFDM Systems,” in *Proc. IEEE VTC Spring 2008*, Marina Bay, Singapore, May 2008, pp. 802–806.

[20] E. Akay, E. Sengul, and E. Ayanoglu, “Performance Analysis of Beamforming for MIMO OFDM with BICM,” in *Proc. IEEE ICC 2005*, vol. 1, Seoul, Korea, May 2005, pp. 613–617.

[21] ——, “MIMO BICM-OFDM Beamforming with Full and Partial CSIT,” in *Proc. IEEE ITA 2007*, San Diego, CA, USA, Jan. 2007, pp. 27–31.

[22] Z. Wang and G. B. Giannakis, “Wireless Multicarrier Communications: Where Fourier Meets Shannon,” *IEEE Signal Process. Mag.*, vol. 17, no. 3, pp. 29–48, May 2000.

[23] D. L. Göeckel and G. Ananthaswamy, “On the Design of Multidimensional Signal Sets for OFDM Systems,” *IEEE Trans. Commun.*, vol. 50, no. 3, pp. 442–452, Mar. 2002.

[24] Z. Liu, Y. Xin, and G. B. Giannakis, “Linear Constellation Precoding for OFDM with Maximum Multipath Diversity and Coding Gains,” *IEEE Trans. Commun.*, vol. 51, no. 3, pp. 416–427, Mar. 2003.

[25] D. Haccoun and G. Begin, “High-Rate Punctured Convolutional Codes for Viterbi and Sequential Decoding,” *IEEE Trans. Commun.*, vol. 37, no. 11, pp. 1113–1125, Nov. 1989.

[26] G. Caire, G. Taricco, and E. Biglieri, “Bit-Interleaved Coded Modulation,” *IEEE Trans. Inf. Theory*, vol. 44, no. 3, pp. 927–946, May 1998.

[27] I. Lee, A. M. Chan, and C.-E. W. Sundberg, “Space-Time Bit-Interleaved Coded Modulation for OFDM Systems,” *IEEE Trans. Signal Process.*, vol. 52, no. 3, pp. 820–825, Mar. 2004.

[28] Z. Liu, Y. Xin, and G. B. Giannakis, “Space-Time-Frequency Coded OFDM over Frequency-Selective Fading Channels,” *IEEE Trans. Signal Process.*, vol. 50, no. 10, pp. 2465–2476, Oct. 2002.

[29] A. Gut, *An Intermediate Course in Probability*, 2nd ed. Springer, 2009.

[30] H. J. Park and E. Ayanoglu, “An Upper Bound to the Marginal PDF of the Ordered Eigenvalues of Wishart Matrices and Its Application to MIMO Diversity Analysis,” in *Proc. IEEE ICC 2010*, Cape Town, South Africa, May 2010.

[31] A. Edelman, “Eigenvalues and condition numbers of random matrices,” Ph.D. dissertation, Massachusetts Institute of Technology, 1989.

[32] O. Edfors, M. Sandell, J.-J. van de Beek, S. K. Wilson, and P. O. Borjesson, “OFDM Channel Estimation by Singular Value Decomposition,” *IEEE Trans. Commun.*, vol. 46, no. 7, pp. 931–939, Jul. 1998.

[33] P. J. Smith and L. M. Garth, “Distribution and Characteristic Functions for Correlated Complex Wishart Matrices,” *Journal of Multivariate Analysis*, vol. 98, p. 661677, Apr. 2007.

[34] P.-H. Kuo, P. J. Smith, and L. M. Garth, “Joint Density for Eigenvalues of Two Correlated Complex Wishart Matrices: Characterization of MIMO Systems,” *IEEE Trans. Wireless Commun.*, vol. 6, no. 11, pp. 3902–3906, Nov. 2007.

[35] M. Chiani, M. Z. Win, and H. Shin, “MIMO Networks: The Effects of Interference,” *IEEE Trans. Inf. Theory*, vol. 56, no. 1, pp. 336–349, Jan. 2010.

[36] Y. Cho, J. Kim, W. Yang, and C. Kang, *MIMO-OFDM Wireless Communications with MATLAB*. Wiley-IEEE Press, 2010.

[37] R. Dilmaghani and M. Ghavami, “Comparison between Wavelet-based and Fourier-based Multicarrier UWB Systems,” *IET Communications*, vol. 2, no. 2, pp. 353–358, Feb. 2008.

[38] K. Abdullah and Z. M. Hussain, “Studies on DWT-OFDM and FFT-OFDM Systems,” in *Proc. ICCCP 2009*, Muscat, Oman, Feb. 2009.

[39] O. Daoud, “Performance Improvement of Wavelet Packet Transform over Fast Fourier Transform in Multiple-Input Multiple-Output Orthogonal Frequency Division Multiplexing Systems,” *IET Communication*, vol. 6, no. 7, pp. 765–773, May 2012.

[40] F. Farrukh, S. Baig, and M. J. Mughal, “Performance Comparison of DFT-OFDM and Wavelet-OFDM with Zero-Forcing Equalizer for FIR Channel Equalization,” in *Proc. ICEE 2007*, Coimbra, Portugal, Sep. 2007.

[41] S. Kiani, S. Baig, and M. J. Mughal, “Overlap Frequency Domain Equalization for Wavelet OFDM,” in *Proc. ITC-CSCC 2009*, Jeju Island, Korea, Jul. 2009, pp. 1346–1349.

[42] U. Khan, S. Baig, and M. J. Mughal, “Performance Comparison of Wavelet Packet Modulation and OFDM over Multipath Wireless Channel with Narrowband Interference,” *International Journal of Electrical & Computer Sciences*, vol. 9, no. 9, pp. 431–434, Oct. 2009.

[43] H. J. Park and E. Ayanoglu, “Constellation Precoded Beamforming,” in *Proc. IEEE GLOBECOM 2009*, Honolulu, HI, USA, Nov. 2009.

[44] ——, “Bit-Interleaved Coded Multiple Beamforming with Constellation Precoding,” in *Proc. IEEE ICC 2010*, Cape Town, South Africa, May 2010.

[45] H. J. Park, B. Li, and E. Ayanoglu, “Multiple Beamforming with Constellation Precoding: Diversity Analysis and Sphere Decoding,” in *Proc. IEEE ITA 2010*, San Diego, CA, USA, Apr. 2010.

[46] ——, “Constellation Precoded Multiple Beamforming,” *IEEE Trans. Commun.*, vol. 59, no. 5, pp. 1275–1286, May 2011.

[47] F. Oggier, G. G. Rekaya, J.-C. Belfiore, and E. Viterbo, “Perfect Space-Time Block Codes,” *IEEE Trans. Inf. Theory*, vol. 52, no. 9, pp. 3885–3902, 2006.

[48] B. Li and E. Ayanoglu, “Golden Coded Multiple Beamfoming,” in *Proc. IEEE GLOBECOM 2010*, Miami, FL, USA, Dec. 2010.

[49] ——, “Bit-Interleaved Coded Multiple Beamforming with Perfect Coding,” in *Proc. IEEE ICC 2012*, Ottawa, Canada, Jun. 2012, to be published.

[50] ——, “Multiple Beamforming with Perfect Coding,” *IEEE Trans. Commun.*, vol. 60, no. 6, pp. 1575–1586, Jun. 2012.